Evaluating the potential use of a dairy industry residue to induce denitrification in polluted water bodies: a flow-through experiment.

Rosanna Margalef-Marti, Raúl Carrey, Albert Soler, Neus Otero

Journal of Environmental Management, 2019, Volume 245, Pages 86-94
DOI: https://doi.org/10.1016/j.jenvman.2019.03.086

Received date: 30 January 2019
Revised date: 15 March 2019
Accepted date: 16 March 2019
Available online: 28 May 2019

Evaluating the potential use of a dairy industry residue to induce denitrification in polluted water bodies: a flow-through experiment.

Rosanna Margalef-Marti[1], Raúl Carrey[1], Albert Soler[1], Neus Otero[1,2]

[1] Grup MAiMA, SGR Mineralogia Aplicada, Geoquímica i Geomicrobiologia, Departament de Mineralogia, Petrologia i Geologia Aplicada, Facultat de Ciències de la Terra, Universitat de Barcelona (UB), Barcelona (Spain).

[2] Serra Húnter Fellowship, Generalitat de Catalunya, Spain.

ABSTRACT

Improving the effectiveness and economics of strategies to remediate groundwater nitrate pollution is a matter of concern. In this context, the addition of whey into aquifers could provide a feasible solution to attenuate nitrate contamination by inducing heterotrophic denitrification, while recycling industry residue. Before its application, the efficacy of the treatment must be studied at the laboratory-scale to optimize the application strategy in order to avoid the generation of harmful intermediate compounds. To do this, a flow-through denitrification experiment using whey as an organic C source was performed, and different C/N ratios and injection periodicities were tested. The collected samples were analyzed to determine the chemical and isotopic composition of N and C compounds. The results proved that whey could promote denitrification. Nitrate was completely removed when using either a 3.0 or 2.0 C/N ratio. However, daily injection with C/N ratios from 1.25 to 1.5 seemed advantageous, since this level decreased nitrate concentration to values below the threshold for water consumption while avoiding nitrite accumulation and whey release with the outflow. The isotopic results confirmed that nitrate attenuation was due to denitrification coupled to the

production of DIC from bacterial whey oxidation. Furthermore, the isotopic data suggested that when denitrification was not complete, the outflow could present a mix of denitrified and nondenitrified water. The calculated isotopic fractionation values ($\varepsilon^{15}N_{NO3/N2}$ and $\varepsilon^{18}O_{NO3/N2}$) might be applied in the future to quantify the efficiency of the bioremediation treatments of whey application at the field-scale.

Keywords: Groundwater, Isotopic Fractionation, Nitrate, Remediation, Whey

1. Introduction

Nitrogen is essential for life, but many compounds such as the oxidized forms nitrate (NO_3^-), nitrite (NO_2^-) and nitrogen oxide (N_2O) have been recognized to produce detrimental effects on human health and the environment (Rivett et al., 2008; Vitousek et al., 1997; Ward et al., 2005). A concentration of 0.8 mM NO_3^- is the threshold value for consumption set in the World Health Organization guidelines for drinking water (WHO, 2011) and the European Drinking Water Directive (98/83/EC, 1998) and the threshold established by the Groundwater Framework Directive (2006/118/EC, 2006) as a goal to achieve good groundwater quality status. At the European level, measures aiming to reduce and prevent NO_3^- pollution from agricultural sources have been applied since 1991, following the Nitrates Directive (91/676/EEC, 1991). However, the last available report from the European Environmental Agency shows, for the period 1992-2012, an overall diminution in NO_3^- content in surface water but a flat trend in groundwater (EEA, 2015). Sebilo et al., (2013) performed a long-term lysimeter study and found that N is retained in soils for up to 30 years and that due to past fertilizer applications, NO_3^- can continue leaching into groundwater for an additional five decades. Consequently, developing remediation strategies and improving their effectiveness and economics is fundamental.

One of the most studied remediation treatments for removing NO_3^- from water is based on the enhancement of denitrification (Khan and Spalding, 2004; Vidal-Gavilan et al.,

2013). Denitrification is the oxidation of an electron donor and subsequent reduction of NO_3^- to harmless gaseous N_2 through a series of enzymatic reactions involving diverse N compounds: $NO_3^- \rightarrow NO_2^- \rightarrow NO \rightarrow N_2O \rightarrow N_2$ (Knowles, 1982). It occurs naturally in the environment if an electron donor is available, if intrinsic denitrifying bacteria are present and if dissolved oxygen concentration is low (Korom, 1992). However, NO_3^- usually persists in groundwater due to electron donor deficiency (Rivett et al., 2008). To overcome this natural limitation, promotion of heterotrophic denitrification based on the addition of external carbon (C) sources within the aquifers has already been implemented and demonstrated to be effective (Borden et al., 2012; Critchley et al., 2014; Leverenz et al., 2010; Smith et al., 2001). The specific electron donor compound employed, as well as the feeding strategy, play a critical role in the resulting efficiency (Vidal-Gavilan et al., 2014).

Pure organic C compounds, such as glucose, acetate, ethanol or methanol, effectively promote heterotrophic denitrification (Akunna et al., 1993; Carrey et al., 2014; Peng et al., 2007). However, since the use of pure compounds might become expensive in long-term treatments, there has been an increasing interest in using alternative organic C sources. The potential use of animal or vegetal waste has already been verified (Grau-Martínez et al., 2017; Trois et al., 2010). However, to promote groundwater remediation within the aquifer, liquid compounds are preferable as they could be easily applied by injection through already constructed wells. In this context, a wine industry residue was recently tested to promote heterotrophic denitrification (Carrey et al., 2018). The use of whey may also be an economically feasible solution to attenuate NO_3^- pollution, while providing waste recycling. To the authors' knowledge, although a few previous studies focused on N removal by lactic acid derived products (Fernández-Nava et al., 2010; Safonov et al., 2018; Sage et al., 2006; Tang et al., 2018), an assessment of whey recycling to promote denitrification by means of isotopic tools has not yet been reported. The dairy industry byproduct has already been demonstrated to be a feasible electron

donor to remove other water contaminants, such as Cr^{6+}, trichloroethylene (TCE) or 2,4,6-trinitrotoluene (TNT) (Innemanová et al., 2015; Mclean et al., 2015; Němeček et al., 2015; Orozco et al., 2010). Furthermore, as whey is considered one of the most important pollutants in dairy industry wastewaters, its reuse would decrease the treatment cost (Carvalho et al., 2013). Before field-scale application, laboratory experiments must be performed to assess the viability of using whey to promote denitrification and to assess the occurrence of adverse effects, such as the accumulation of undesirable intermediates or clogging due to a biomass increase (Rodríguez-Escales et al., 2016; Vidal-Gavilan et al., 2014).

Chemical and isotopic characterization has been widely applied to trace natural and induced NO_3^- transformation processes (Aravena and Robertson, 1998; Vidal-Gavilan et al., 2013). In the course of denitrification, unreacted residual NO_3^- becomes enriched in the heavy isotopes ^{15}N and ^{18}O, permitting the differentiation of biological attenuation from other processes, such as dilution, that have no influence on the isotopic signature (Böttcher et al., 1990). The observed isotopic fractionation (ε) of N and O from dissolved NO_3^- can be used to estimate the efficacy of induced denitrification (Mariotti et al., 1988). Furthermore, the isotopic characterization ($\delta^{13}C$) of dissolved organic and inorganic carbon (DOC and DIC) during denitrification might provide knowledge on the fate of the added organic C source (Carrey et al., 2018; Nascimento and Krishnamurthy, 1997).

This work aims to evaluate the suitability of whey to promote heterotrophic denitrification if injected into NO_3^- polluted aquifers. The present study investigates the best strategy to reduce NO_3^- values below the threshold fixed by European Directives, as well as the best strategy to achieve complete whey consumption while preventing the generation of adverse compounds, such as NO_2^-, or excessive biomass. To reach the goal, the response to modifications to the C/N ratio or injection periodicity were assessed by means of a laboratory flow-through experiment. The isotopic composition of N and O

from dissolved NO_3^- and C from DOC and DIC were determined throughout the experiment and were discussed along with the chemical characterization.

2. Materials and methods

2.1. Experimental setup

The flow-through experiment was performed simulating aquifer conditions. Synthetic water was prepared with an approximate NO_3^- concentration of 1.9 mM, which was maintained throughout the experiment. The specific chemical composition of the inflow water is shown as supporting information (**Table S1**).

Synthetic water from the inflow reservoir (2000 mL) flowed from the bottom to the top of a glass column (70 cm long, 8 cm diameter) and was discharged into the outflow reservoir (500 mL). Flow rate was maintained at a constant rate of 0.2 mL/min by using a peristaltic pump (Micropump Reglo digital, 4 channels, ISMATEC). The glass column was filled with silica balls (5 mm diameter) to provide a homogenous porous medium; the total volume was 3.5 L and the water volume was 1.2 L. To monitor the Eh and pH evolution, probes were installed between the column and the outflow container, and values were recorded hourly. All components of the experimental system were connected by Tygon tubes and were installed inside a temperature-regulated chamber set at 14 °C, except the inflow container. Eight sampling points were established: one at the inflow container, six along the glass column at 10 cm intervals (VP1 to VP6) and one at the outflow container. The injection was performed through three injection points located at the same height as the sampling point PV2, near the bottom of the column (**Figure 1**).

Before biostimulation (described in section 2.2), an initial operation period with no electron donor injection was carried out in order to assess the system performance (Stage 0). During this initial operation period, a bromide tracer test was conducted to

determine the hydraulic parameters of the column. The average water residence time in the column was estimated to be approximately 4 days.

2.2. Electron donor supply

Whey (from ecological stockbreeding) was used as the unique electron donor source to promote heterotrophic denitrifying bacterial growth. The determined nonpurgeable dissolved organic C (NPDOC) and total organic C (TOC) in whey were 2.15 M and 2.48 M, respectively. As whey is known to usually contain a certain amount of NO_3^- (Oliveira et al., 1995), it was assumed that it would also serve as the denitrifying bacteria inoculum. The used whey had NO_3^- and NO_2^- concentrations (determined by high-performance liquid chromatography (HPLC)) of 0.03 mM and 0.14 mM, respectively. Its contribution was considered insignificant in the experiment compared to the synthetic water's initial NO_3^- concentration (1.9 mM) and considering the low volume injected (between 0.25 and 3 mL).

After Stage 0, different feeding strategies (Stages I to VI) were tested by injecting whey in varying C/N ratios and periodicities. The molar C/N ratio was calculated according to the total NPDOC measured in whey. The initial parameters were set according to the literature data and then optimized based on the obtained results. Throughout Stage I, the injection was carried out every 4 days at a 3.0 C/N ratio. Throughout Stages III, IV and V, a daily injection was tested with 2.0, 1.5 and 1.25 C/N ratios, respectively. Stages II and VI, which had no injection, were used to assess the running period of the treatment. The experiment ran for almost 5 months, and samples were periodically obtained according to each stage's purpose. All stages are summarized in **Table 1**.

2.3. Analytical methods

All samples were immediately filtered when obtained through a 0.2 µm Millipore® filter and stored at 4 °C until analysis, except aliquots for isotopic characterization of N and O

of dissolved NO_3^- that were preserved frozen at -20 °C. Aliquots with no headspace were stored for organic and inorganic C concentration and isotopic composition determination.

Major anions (Cl^-, NO_2^-, NO_3^- and SO_4^{2-}) were analyzed by HPLC (WATERS 515 pump and WATERS IC-PAK ANIONS column with WATERS 432 and UV/V KONTRON detectors); NH_4^+ was determined by spectrophotometry using the indophenol blue method (CARY 1E UV-visible); DIC was measured by titration (METROHM 702 SM Titrino); NPDOC was analyzed by the organic matter combustion method (TOC 500 SHIMADZU); major cations were determined by ICP-OES (Perkin Elmer Optima 8300) and trace elements by ICP-MS (Perkin Elmer Elan 6000).

The $\delta^{15}N\text{-}NO_3^-$ and $\delta^{18}O\text{-}NO_3^-$ were determined following the cadmium reduction method (McIlvin and Altabet, 2005; Ryabenko et al., 2009). The N_2O was analyzed using a Pre-Con (Thermo Scientific) coupled to a Finnigan MAT 253 Isotope Ratio Mass Spectrometer (IRMS, Thermo Scientific). The $\delta^{13}C$-DIC was analyzed by carbonate conversion to CO_2 gas by adding a phosphoric acid solution and measurement using a Gas-Bench II coupled to a MAT-253 IRMS (Thermo Scientific). The $\delta^{13}C$-DOC was determined by HPLC-IRMS (Delta V ADVANTAGE, Thermo-Finnigan). Notation is expressed in terms of δ ‰ ($\delta = ((R_{sample}-R_{standard})/R_{standard})$, where R is the ratio between the heavy and the light isotopes). The international standards used in this study were: AIR (Atmospheric N_2) for $\delta^{15}N$, V-SMOW (Vienna Standard Mean Oceanic Water) for $\delta^{18}O$ and V-PDB (Vienna Peedee Belemnite) for $\delta^{13}C$. According to (Coplen, 2011), several international and laboratory standards were interspersed among samples for normalization of analyses. Three international standards (USGS 32, 34 and 35) and one internal laboratory standard (CCIT-IWS ($\delta^{15}N$ = +16.9 ‰ and $\delta^{18}O$ = +28.5 ‰)) were employed to correct $\delta^{15}N\text{-}NO_3^-$ and $\delta^{18}O\text{-}NO_3^-$ values; three internal laboratory standards (CCIT-NaHCO3 ($\delta^{13}C$ = -4.4 ‰), CCIT-NaKHCO3 ($\delta^{13}C$ = -18.7 ‰) and CCIT-KHCO3 ($\delta^{13}C$ = +29.2 ‰)) to correct $\delta^{13}C$-DIC analyses; and one international standard (IAEA-CH6) and two internal laboratory standards (CCIT-Gly ($\delta^{13}C$ = -30.8 ‰) and CCIT-

UCGEMA ($\delta^{13}C$ = -24.8 ‰)) to correct $\delta^{13}C$-DOC results. The reproducibility (1σ) of the samples, calculated from the standards systematically interspersed in the analytical batches, was ±1.0 ‰ for $\delta^{15}N$-NO_3^-, ±1.5 ‰ for $\delta^{18}O$-NO_3^-, ±0.2 ‰ for $\delta^{13}C$-DIC and ±0.3 ‰ for $\delta^{13}C$-DOC.

Chemical and isotopic analyses were prepared at the laboratory of the MAiMA-UB research group and analyzed at the Centres Científics i Tecnològics of the Universitat de Barcelona (CCiT-UB).

3. Results and discussion

3.1. NO_3^- attenuation promoted by whey injections

The chemical and isotopic composition of N and C compounds from the samples collected throughout the experiment are reported in supporting information, **Table S2**. The pH and Eh recorded hourly from Stage I to V are presented in supporting information, **Figure S1**. While the pH values averaged 7.4 and did not show significant variations along the experiment, the Eh fluctuated from +515 to -345 mV, demonstrating that the whey injections promoted the reducing conditions needed for denitrification. Two days after the first injection in Stage I (injection every four days at a 3.0 C/N ratio), NO_3^- attenuation began and NO_2^- accumulated, reaching 1.5 mM (NO_3^- in the inflow along the experiment was 1.9 ± 0.2 mM). After the peak, NO_2^- started to decrease until both compounds were completely depleted in less than sixteen days from the beginning of the biostimulation strategy (**Figure 2**). The lag-phase was short, possibly because significant denitrifying bacterial species were intrinsically present in whey, as it usually contains traces of N compounds (Oliveira et al., 1995). Tang et al. (2018) after inducing denitrification by addition of lactate observed a high microbial diversity encompassed by a diversification on metabolic pathways which even increased when using a complex C source rich in lactic acid. The stimulated bacterial community in the present experiment was not determined since it was not a main goal in the paper, on future field-scale

applications, the bacterial community might vary from site to site. In addition to denitrification, the observed NO_3^- reduction could have been promoted by the dissimilatory NO_3^- reduction to ammonium (DNRA). However, during the experiment, NH_4^+ was rarely detected during Stages I, II and III, with concentrations below 0.19 mM. This suggests that denitrification was the main NO_3^- removal process and that DNRA did not contribute significantly to NO_3^- attenuation. After a period with no injection, where NO_3^- concentration progressively increased to the initial values (Stage II), the injection strategy was switched to a daily injection with a 2.0 C/N ratio (Stage III). During Stage III, NO_3^- was also rapidly and completely reduced but with no NO_2^- accumulation. In a similar study, no NO_2^- accumulated during a daily injection strategy using a 2.5 C/N ratio tested after a weekly injection strategy that presented NO_2^- values up to 0.7 mM (initial NO_3^- was 1.6 mM) (Vidal-Gavilan et al., 2014). The lack of NO_2^- accumulation during the daily injection strategy was likely due to the latent denitrifying community during the recovery period that quickly adapted when the injections were resumed compared to the beginning of the biostimulation.

During Stages I and III, complete NO_3^- reduction was achieved since the electron donor was in excess. In the following injection periods, lower C/N ratios were tested with a daily injection strategy. With a 1.25 C/N ratio (Stage IV), NO_3^- in the outflow was maintained at approximately 0.5 mM, and with a 1.5 C/N ratio (Stage V), NO_3^- decreased to approximately 0.4 mM. The slight NO_3^- concentration fluctuations observed during Stages IV and V were due to system instability caused by clogging derived from biomass accumulation inside the tubes. Biomass accumulation began at the end of Stage I but increased significantly during the following stages. In a wastewater treatment study, lowering the C/N ratio from 20 to 4 favored a poor flocculation and settleability, which resulted in a higher effluent turbidity and suspended solids (Ye et al., 2011). These results are in accordance with the observed biomass migration across the column and tubes in our experiment and in a similar laboratory biostimulation study performed by

(Carrey et al., 2018). The long persistence of denitrification during the recovery Stage II was a demonstration of the excessive organic C supplied during Stage I and suggested the possible use of biomass as a secondary organic C pool, since biomass has been observed to be the main electron donor source at low C/N ratios in a similar flow-through experiment (Carrey et al., 2018). After the last whey injection in Stage I, five days were needed to reach NO_3^- levels above the detection limit, and forty days were needed to equal the inflow water NO_3^- concentration. In contrast, the recovery period in Stage VI lasted just eleven days due to the higher initial NO_3^- concentration (approximately 0.5 mM) and the lower C/N ratio. The lower C/N ratio could have also decreased the availability of biomass as a secondary C source during Stage VI compared to Stage II due to the aforementioned promotion of biomass migration and loss with the outflow.

Vertical profile samples were useful in assessing the denitrification process along the column. After biostimulation, both in the case of complete (Stage I) and partial (Stage V) denitrification, a sharp NO_3^- decrease was observed at the bottom of the column, near and below the injection point (16 cm) (**Figure 3**). Following the redox sequence, dissolved oxygen from the inflow water should be consumed before NO_3^- is used as an electron acceptor. Therefore, NO_3^- attenuation was expected to be observed above the injection points rather than below. Possibly because whey is denser than water, part of the whey might have accumulated at the bottom of the column, thereby increasing the C/N ratio in the first centimeters of the column, which may have led to strong reducing conditions and, consequently, made the NO_3^- attenuation start below the injection points. This fact should be taken into account in future field-scale applications since whey could flow down to the bottom part of the aquifer due to these density differences. Contrarily, during the recovery period (Stage II), NO_3^- was progressively reduced along the column. Conclusions concerning the NO_2^- distribution within the column could not be made since no NO_2^- accumulation was detected when the vertical profile samples were obtained.

3.2. NO_3^- isotopic characterization

Under closed system conditions, the ε can be modeled using a Rayleigh distillation **Equation 1**. In this way, the ε is obtained from the slope of the linear correlation between the natural logarithm of the substrate remaining fraction ($Ln(C_{residual}/C_{initial})$, where C refers to analyte concentration) and the determined isotope ratios ($Ln(R_{residual}/R_{initial})$, where $R = (\delta+1)$). Despite the column being an open system, as the electron donor and acceptor were replenished, it was assumed that during the injection periods with excess C/N ratios (Stages I and III), the isotopic composition of outflow NO_3^- was solely influenced by the NO_3^- bacterial reduction. The treatment homogeneity was demonstrated by the vertical profile results, showing complete denitrification at the bottom of the column that allowed to discard a mix of treated and nontreated synthetic water at the outflow container. Therefore, we considered it appropriate to use the Rayleigh model to calculate the ε during the biostimulation Stages I and III. Previous studies have demonstrated equal isotopic fractionation between batches and similar flow-through induced denitrification experiments (R. Carrey et al., 2014; Grau-Martínez et al., 2017). However, for the recovery (II, VI) and partial denitrification stages (IV, V), a possible mix between denitrified and nondenitrified water could not be discarded and for this reason, the Rayleigh equation was not applied.

$$Ln\left(\frac{R_{residual}}{R_{initial}}\right) = \varepsilon \times Ln\left(\frac{C_{residual}}{C_{initial}}\right) \quad (\textbf{Equation 1})$$

As expected for the NO_3^- biological reduction, a linear correlation between the $\delta^{15}N\text{-}NO_3^-$ and $\delta^{18}O\text{-}NO_3^-$ and the Ln of the remaining NO_3^- concentration was observed in the stages that achieved complete NO_3^- removal (Stages I and III). During both stages, the isotopic composition increased from values of the synthetic water ($\delta^{15}N\text{-}NO_3^-$ = +16.7 ‰ and $\delta^{18}O\text{-}NO_3^-$ = +28.4 ‰) to values up to $\delta^{15}N\text{-}NO_3^-$ = +45.8 ‰ and $\delta^{18}O\text{-}NO_3^-$ = +77.3 ‰ during Stage I and up to $\delta^{15}N\text{-}NO_3^-$ = +31.7 ‰ and $\delta^{18}O\text{-}NO_3^-$ = +39.6 ‰ during Stage III. The calculated $\varepsilon^{15}N_{NO3/N2}$ and $\varepsilon^{18}O_{NO3/N2}$ were -10.9 ‰ and -16.3 ‰, respectively, for Stage I and -8.6 ‰ and -5.5 ‰, respectively, for Stage III (**Figures 4A and 4B**). The resulting $\varepsilon^{15}N/\varepsilon^{18}O$ was 0.7 for Stage I and 1.6 for Stage III. Nevertheless, during the

partial denitrification stages (Stages IV and V), no correlation was observed between the isotopic composition and the Ln of the NO_3^- concentration (**Figures 4C and 4D**) or 1/[NO_3^-] (supporting information, **Figure S2**). The isotopic values during these stages were close to the synthetic water isotopic composition. For the recovery stages (Stages II and VI), a correlation between the Ln of the remaining NO_3^- concentration and the isotopic composition was again observed (**Figures 4C and 4D**). However, the resulting trend from plotting δ^{15}N-NO_3^- and δ^{18}O-NO_3^- versus 1/[NO_3^-] was better adjusted to a linear correlation than to a logarithmic trend (supporting information, **Figure S2**), which is indicative of mixing processes. These results suggested a mix of denitrified and nondenitrified water at the outflow during the recovery and partial denitrification periods.

During the experiment, the NO_3^- isotopic fractionation could have been influenced by several factors. The $\varepsilon^{15}N_{NO3/N2}$ and $\varepsilon^{18}O_{NO3/N2}$ might depend on the enzymes involved in the NO_3^- reduction, the NO_3^- transport across the cell and the NO_3^- reduction rate, while factors such as the pH or salinity do not seem to provoke significant effects (Granger et al., 2008; Wunderlich et al., 2012). Due to the use of different initial electron donor and acceptor concentrations among the tested stages, the ratio of cellular NO_3^- uptake and efflux before the enzymatic reaction and the NO_3^- reduction rate was expected to play a role in the variability in the $\varepsilon^{15}N_{NO3/N2}$ and $\varepsilon^{18}O_{NO3/N2}$ results. Furthermore, a shift in the $\varepsilon^{15}N/\varepsilon^{18}O$ ratio with respect to 1, the typical recognized value for denitrification, can be attributed to (I) NO_2^- reoxidation to NO_3^- (Buchwald and Casciotti, 2010; Granger and Wankel, 2016; Wunderlich et al., 2013); (II) NH_4^+ oxidation to NO_3^- (Bourbonnais et al., 2013; Dähnke and Thamdrup, 2016; Granger and Wankel, 2016) and (III) major activity of bacteria containing the periplasmic NO_3^- reductase (NAP) instead of the membrane-bound NO_3^- reductase (NAR) (Granger et al., 2008). For this reason, $\varepsilon^{15}N/\varepsilon^{18}O$ values close to 2 are usually found in field-scale freshwater denitrification studies (Critchley et al., 2014; Otero et al., 2009), while values remain close to 1 in laboratory experiments performed under controlled closed conditions (Carrey et al., 2013; Grau-Martínez et al.,

2017). NAP is not expected to be of great significance, since it is not a respiratory enzyme and it is not associated with energy production (Granger et al., 2008 and references therein), and NH_4^+ was rarely detected throughout all the experimental stages. Hence, the most likely explanation for the higher calculated $\varepsilon^{15}N/\varepsilon^{18}O$ value for Stage III (1.6, $r^2 = 0.87$) compared to Stage I (0.7, $r^2 = 0.96$) is the occurrence of NO_2^- reoxidation, since a higher O_2 diffusion into the system was expected during Stage III due to daily injections compared to the decreased periodicity in Stage I. However, other explanations cannot be completely ruled out. I influence of the important N assimilation that took place in Stage I also needs to be considered because of the initial biostimulation and the mix between denitrified and nondenitrified groundwater that occurred during the recovery and partial denitrification stages.

3.3. Whey consumption

NPDOC results showed organic C consumption coupled with NO_3^- reduction. The highest NPDOC concentration at the outflow was observed at the beginning of Stage I but was also significant at the beginning of Stage III (4.9 and 1.6 mM C, respectively, while injected whey was 5.1 and 3.4 mM C, respectively). The initial lack of organic C decrease at the outflow with respect to the injected whey can be explained by the time needed for the establishment of the bacterial community. After the acclimation period of 2 days, NPDOC peaks in the outflow of the column derived from injections decreased progressively (**Figure 5**). Apart from the injected electron donor, the organic C resulting from bacterial metabolism, biomass degradation and cellular lysis could also act as a secondary electron donor source, especially at low C/N ratios (Carrey et al., 2018).

The HCO_3^- showed an inverse trend compared to the NO_3^- concentration as expected from heterotrophic denitrification (**Equation 2**). The DIC concentration started to increase 5 days after the beginning of injections, with maximum values coinciding with complete NO_3^- depletion at Stages I and III (4.0 and 4.1 mM C, respectively, compared

to the background C of 1.8 mM), and its production stopping during the recovery Stage II (**Figure 5**). The gap between C derived from injected whey and the sum of the outflow DIC and NPDOC was attributed to biomass and CO_2 production.

$4NO_3^- + 5C_{org} + 2H_2O \rightarrow 2N_2 + 4HCO_3^- + CO_2$ (**Equation 2**)

Denitrification studies that include C isotopic characterization are still scarce, likely because it is difficult to separate all the intricate pathways involved in the process. At the beginning of this study (between the second and third injections), as NPDOC in the outflow decreased due to electron donor consumption, the remaining DOC became enriched in $\delta^{13}C$ (**Figure 5**). The isotopic fractionation was likely caused because bacteria preferentially consumed the lighter C molecules, leading to an isotopic increase from $\delta^{13}C$-DOC values close to the isotopic composition of whey (-28 ‰) to $\delta^{13}C$-DOC values in the outflow up to -15 ‰ (**Figure 5**). It must be considered that not only whey and its enzymatic oxidation influence the $\delta^{13}C$-DOC results, since the organic C resulting from bacterial metabolism, biomass degradation or cell lysis events introduces variations in the global $\delta^{13}C$-DOC (Carrey et al., 2018). The $\delta^{13}C$ results only covered the first ten days of Stage I; therefore, it could be assumed that no biomass degradation or cell lysis events occurred, and bacterial biomass organic C pool contribution was negligible in this period. Thus, the observed C isotopic fractionation was related to the enzymatic oxidation of whey. The slope of the regression line between $\delta^{13}C$-DOC and Ln[NPDOC] was -7 ‰ (r^2 = 0.66) (**Figure 6A**).

Regarding HCO_3^- production during Stage I, as DIC concentration increased, it became depleted in $\delta^{13}C$ (-17 ‰), while during Stage II (recovery period), the $\delta^{13}C$-DIC was progressively enriched and coupled to a concentration decrease until both concentration and isotopic composition reached the initial synthetic water values (-8 ‰) (**Figure 5**). Both the $\delta^{13}C$-DIC and DIC concentration remained mainly constant at partial denitrification Stages IV and V. The measured $\delta^{13}C$-DIC at the outflow samples is a mix

between the $\delta^{13}C$ of the inflow water DIC (-9 ‰) and the DIC produced from whey oxidation. For this reason, $\delta^{13}C$-DIC is influenced by the $\delta^{13}C$ of whey (-28 ‰), the isotopic fractionation produced during bacterial metabolism, and could be affected by the equilibrium between the $CO_2(aq)$, HCO_3^- and CO_3^{2-} species (Blaser and Conrad, 2016; Mariotti, 1991). Observing the isotopic results obtained at each period, a nearly linear correlation between $\delta^{13}C$-DIC and Ln[DIC] was observed during Stages II (recovery) and III (complete denitrification period), giving a slope of -8 ‰ (r^2 = 0.94) (**Figure 6B**). However, a nonlinear trend was found for Stage I. The reason could be a higher isotopic fractionation produced between the microbial organic C pool and the generated DIC during the beginning of Stage I that accounted for most of the biomass generation throughout the study compared to the following stages. In fact, from the middle to the end of Stage I, a line with a parallel trend to the linear correlation obtained for Stages II and III was observed. The results obtained for the few samples collected throughout the partial denitrification Stages IV and V fell at the lower extreme of the regression line plotted for Stages II and III. This can be explained by a higher influence of the inflow water $\delta^{13}C$-DIC on the outflow $\delta^{13}C$-DIC, since during the partial denitrification stages, a lower amount of DIC was produced compared to Stages I and III.

3.4. Suitability for field-scale application

Thinking about this experiment in terms of achieving safe drinking water, semiquantitative ICP analysis in selected outflow water samples was performed to discard possible trace elements released from whey injections. As no toxic elements were observed to be released and given the results discussed above, whey was considered to be a safe electron donor to promote denitrification in polluted aquifers (supporting information, **Table S3**). For field-scale application, it is recommended to use whey from ecological stockbreeding to avoid the release of antibiotic and hormone residues to the aquifer. Promotion of bacterial metabolic pathways such as DNRA (discussed in section 3.1) or bacterial SO_4^{2-} reduction (BSR), that could also decrease

the water quality by generating hydrogen sulphide, were also discarded. Denitrification and BSR can occur simultaneously, especially at high C/N ratios (Laverman et al., 2012), and whey has already been reported to promote BSR (Christensen et al., 1996). Throughout the present experiment, the SO_4^{2-} concentration did not show significant variations, suggesting that the excess of organic C did not lead to BSR. Therefore, the C/N ratios and injection strategies tested in the present study are considered appropriate in terms of being applied in future field-scale projects aiming to remediate NO_3^- polluted groundwater. Furthermore, the release of the greenhouse gases (GHG) CO_2, CH_4 and N_2O during N and C cycling processes has become a matter of concern. In denitrification strategies, parameters such as the water O_2 concentration, the C/N ratio and the temperature might play an important role in GHG emissions (Miettinen et al., 2015; Spoelstra et al., 2010; Teiter and Mander, 2005). In a study to assess N_2O emissions during the heterotrophic denitrification, a lower accumulation was found in laboratory incubations compared to field (Weymann et al., 2010). These authors attributed the discrepancy to sampling and storage procedures and to differences in the dissolved O_2 concentration and the spatial scale. Although the transferability of the laboratory results to field seems to be limited, determining the GHG production in future laboratory studies should be considered aiming to find biostimulation strategies that lowers GHG emissions. Furthermore, in future field-scale induced denitrification tests, monitoring these GHG is needed to check the contribution to global climate change.

Whey could be easily injected through already constructed wells to promote in situ groundwater denitrification in contaminated aquifers, in contrast to solid compounds that might require application through passive systems, such as permeable reactive barriers (Gibert et al., 2008; Huang et al., 2015; Robertson et al., 2008). The following studies of in situ biostimulation by different electron donor supply strategies could be taken as references and could be improved upon: injection through wells placed across the path of the contaminant plume (Tartakovsky et al., 2002); injection through a daisy-like well

system (Khan and Spalding, 2004); cross-injection through wells perpendicular to the flow direction (Critchley et al., 2014; Gierczak et al., 2007); injection through infiltration galleries (Salminen et al., 2014); or even pumping groundwater, mixing it with an electron donor in a tank and reinjecting it through wells (Vidal-Gavilan et al., 2013). Another option could be the supply of electron donor at the inlet of a constructed wetland to enhance denitrification (Lin et al., 2002). The advantages and disadvantages of each strategy must be carefully evaluated, and previous hydrogeochemical characterization at the field-scale is crucial to succeed in the operational design. Once a strategy is implemented, the calculated $\varepsilon^{15}N_{NO3/N2}$ and $\varepsilon^{18}O_{NO3/N2}$ in the present experiment could be applied to evaluate the efficiency of the bioremediation treatment, as has been done in previous studies (Vidal-Gavilan et al., 2013). However, attention must be focused on hydrogeochemical effects, such as mixing, dilution or rainfall events, which could influence the results and, thus, hinder the evaluation of the remediation strategy performance. For this reason, coupling isotopic approximation with all possible data obtained throughout the characterization process will provide a more accurate evaluation.

4. Conclusions

Whey can be used as a sustainable electron donor source for groundwater remediation, as it has been demonstrated to effectively promote denitrification. Thus, manufacturing waste could be transformed into profit. A daily injection strategy seems to avoid NO_2^- accumulation, and C/N ratios of approximately 1.25 or 1.5 are enough to reach NO_3^- concentrations below the threshold for water consumption, while avoiding excess organic C in the effluent, which is advantageous from the perspective of achieving complete whey consumption. However, biomass presence in the water flow due to a decreased settleability at low C/N ratios must be controlled if applied at the field-scale to avoid clogging issues. The NO_3^- isotopic characterization confirmed that complete NO_3^- removal achieved at Stages I and III was due to denitrification and suggested that at

partial denitrification stages (IV and V) and at recovery stages (II and VI), the outflow could contain a mix of denitrified and nondenitrified water. The calculated $\varepsilon^{15}N_{NO3/N2}$ and $\varepsilon^{18}O_{NO3/N2}$ of NO_3^- might be applied in future field studies to quantify the efficiency of bioremediation treatments. Using $\delta^{13}C$ analyses might help in assessing the fate of electron donor consumption, as C isotopic composition of products, such as DIC or biomass, is clearly influenced by substrate $\delta^{13}C$ and the isotopic fractionation produced throughout the enzymatic activity. From our results, we observed the bacterial preferential consumption of lighter C molecules, as observed for NO_3^-, and a trend of the produced $\delta^{13}C$-DIC towards the $\delta^{13}C$-DOC of the injected whey. However, the complexity of the bacterial metabolism that can involve diverse pathways of catabolic and anabolic processes and the lack of continuity of the $\delta^{13}C$-DOC analysis hindered the interpretation of the $\delta^{13}C$ results.

ACKNOWLEDGEMENTS

This work was financed by the projects: REMEDIATION (CGL2014-57215-C4) and PACE-ISOTEC (CGL2017-87216-C4-1-R), both financed by the Spanish Government and the AEI/FEDER from the EU, and MAG (2017 SGR 1733) from the Catalan Government. Margalef-Marti, R. would like to thank the Spanish Government for the Ph.D. grant BES-2015-072882. We would also like to thank the CCiT of the Universitat de Barcelona for the analytical support.

REFERENCES

2006/118/EC, 2006. Groundwater Directive. Council Directive 2006/118/EC, of 12 December 2006, on the protection of groundwater against pollution and deterioration [WWW Document]. Off. J. Eur. Comm. URL http://ec.europa.eu/environment/index_en.htm (accessed 4.9.17).

91/676/EEC, 1991. Nitrates Directive. Council Directive 91/676/EEC of 12 December 1991, concerning the protection of waters against pollution caused by nitrates

from agricultural sources. [WWW Document]. Off. J. Eur. Comm. URL http://ec.europa.eu/environment/index_en.htm (accessed 4.9.17).

98/83/EC, 1998. Drinking Water Directive. Council Directive 98/83/EC, of 3 November 1998, on the quality of water intended for human consumption. [WWW Document]. Off. J. Eur. Comm. URL http://ec.europa.eu/environment/index_en.htm (accessed 4.9.17).

Akunna, J.C., Bizeau, C., Moletta, R., 1993. Nitrate and nitrite reductions with anaerobic sludge using various carbon sources: Glucose, glycerol, acetic acid, lactic acid and methanol. Water Res. 27, 1303–1312. https://doi.org/10.1016/0043-1354(93)90217-6

Aravena, R., Robertson, W.D., 1998. Use of multiple isotope tracers to evaluate denitrification in ground water: study of nitrate from a large-flux septic system plume. Ground Water 36, 975–982.

Blaser, M., Conrad, R., 2016. Stable carbon isotope fractionation as tracer of carbon cycling in anoxic soil ecosystems. Curr. Opin. Biotechnol. 41, 122–129. https://doi.org/10.1016/j.copbio.2016.07.001

Borden, A.K., Brusseau, M.L., Carroll, K.C., McMillan, A., Akyol, N.H., Berkompas, J., Miao, Z., Jordan, F., Tick, G., Waugh, W.J., Glenn, E.P., 2012. Ethanol addition for enhancing denitrification at the uranium mill tailing site in Monument Valley, AZ. Water. Air. Soil Pollut. 223, 755–763. https://doi.org/10.1007/s11270-011-0899-1

Böttcher, J., Strebel, O., Voerkelius, S., Schmidt, H.-L., 1990. Using isotope fractionation of nitrate-nitrogen and nitrate-oxygen for evaluation of microbial denitrification in a sandy aquifer. J. Hydrol. 114, 413–424. https://doi.org/10.1016/0022-1694(90)90068-9

Bourbonnais, A., Lehmann, M.F., Hamme, R.C., Manning, C.C., Juniper, S.K., 2013. Nitrate elimination and regeneration as evidenced by dissolved inorganic nitrogen isotopes in Saanich Inlet, a seasonally anoxic fjord. Mar. Chem. 157, 194–207. https://doi.org/10.1016/j.marchem.2013.09.006

Buchwald, C., Casciotti, K.L., 2010. Oxygen isotopic fractionation and exchange during bacterial nitrite oxidation. Limnol. Oceanogr. 55, 1064–1074. https://doi.org/10.4319/lo.2010.55.3.1064

Carrey, R., Otero, N., Soler, A., Gómez-Alday, J.J., Ayora, C., 2013. The role of Lower Cretaceous sediments in groundwater nitrate attenuation in central Spain: Column experiments. Appl. Geochemistry 32, 142–152. https://doi.org/10.1016/j.apgeochem.2012.10.009

Carrey, R., Otero, N., Vidal-Gavilan, G., Ayora, C., Soler, A., Gómez-Alday, J.J., 2014. Induced nitrate attenuation by glucose in groundwater: Flow-through experiment. Chem. Geol. 370, 19–28. https://doi.org/10.1016/j.chemgeo.2014.01.016

Carrey, R., Rodríguez-Escales, P., Otero, N., Ayora, C., Soler, a., Gómez-Alday, J.J., 2014. Nitrate attenuation potential of hypersaline lake sediments in central Spain: Flow-through and batch experiments. J. Contam. Hydrol. 164, 323–337. https://doi.org/10.1016/j.jconhyd.2014.06.017

Carrey, R., Rodríguez-Escales, P., Soler, A., Otero, N., 2018. Tracing the role of endogenous carbon in denitrification using wine industry by-product as an external electron donor: Coupling isotopic tools with mathematical modeling. J. Environ. Manage. 207, 105–115. https://doi.org/10.1016/j.jenvman.2017.10.063

Carvalho, F., Prazeres, A.R., Rivas, J., 2013. Cheese whey wastewater: Characterization and treatment. Sci. Total Environ. 445–446, 385–396. https://doi.org/10.1016/j.scitotenv.2012.12.038

Christensen, B., Laake, M., Lien, T., 1996. Treatment of acid mine water by sulfate-reducing bacteria. Results from a bench scale experiment. Water Res. 30, 1617–1624. https://doi.org/10.1016/0043-1354(96)00049-8

Coplen, T.B., 2011. Guidelines and recommended terms for expression of stable-isotope-ratio and gas-ratio measurement results. Rapid Commun. Mass Spectrom. 25, 2538–2560. https://doi.org/10.1002/rcm.5129

Critchley, K., Rudolph, D.L., Devlin, J.F., Schillig, P.C., 2014. Stimulating in situ denitrification in an aerobic, highly permeable municipal drinking water aquifer. J. Contam. Hydrol. 171, 66–80. https://doi.org/10.1016/j.jconhyd.2014.10.008

Dähnke, K., Thamdrup, B., 2016. Isotope fractionation and isotope decoupling during anammox and denitrification in marine sediments. Limnol. Oceanogr. 61, 610–624. https://doi.org/10.1002/lno.10237

European Environment Agency (EEA), 2015. Nutrient trend [WWW Document]. URL https://www.eea.europa.eu/ (accessed 2.5.18).

Fernández-Nava, Y., Marañón, E., Soons, J., Castrillón, L., 2010. Denitrification of high nitrate concentration wastewater using alternative carbon sources. J. Hazard. Mater. 173, 682–688. https://doi.org/10.1016/j.jhazmat.2009.08.140

Gibert, O., Pomierny, S., Rowe, I., Kalin, R.M., 2008. Selection of organic substrates as potential reactive materials for use in a denitrification permeable reactive barrier (PRB). Bioresour. Technol. 99, 7587–7596. https://doi.org/10.1016/j.biortech.2008.02.012

Gierczak, R., Devlin, J.F., Rudolph, D.L., 2007. Field test of a cross-injection scheme for stimulating in situ denitrification near a municipal water supply well. J. Contam. Hydrol. 89, 48–70. https://doi.org/10.1016/j.jconhyd.2006.08.001

Granger, J., Sigman, D.M., Lehmann, M.F., Tortell, P.D., 2008. Nitrogen and oxygen

isotope fractionation during dissimilatory nitrate reduction by denitrifying bacteria. Limnol. Oceanogr. 53, 2533–2545. https://doi.org/10.4319/lo.2008.53.6.2533

Granger, J., Wankel, S.D., 2016. Isotopic overprinting of nitrification on denitrification as a ubiquitous and unifying feature of environmental nitrogen cycling. Proc. Natl. Acad. Sci. 113, E6391–E6400. https://doi.org/10.1073/pnas.1601383113

Grau-Martínez, A., Torrentó, C., Carrey, R., Rodríguez-Escales, P., Domènech, C., Ghiglieri, G., Soler, A., Otero, N., 2017. Feasibility of two low-cost organic substrates for inducing denitrification in artificial recharge ponds: Batch and flow-through experiments. J. Contam. Hydrol. 198, 48–58. https://doi.org/10.1016/j.jconhyd.2017.01.001

Huang, G., Huang, Y., Hu, H., Liu, F., Zhang, Y., Deng, R., 2015. Remediation of nitrate-nitrogen contaminated groundwater using a pilot-scale two-layer heterotrophic-autotrophic denitrification permeable reactive barrier with spongy iron/pine bark. Chemosphere 130, 8–16. https://doi.org/10.1016/j.chemosphere.2015.02.029

Innemanová, P., Velebová, R., Filipová, A., Čvančarová, M., Pokorný, P., Němeček, J., Cajthaml, T., 2015. Anaerobic in situ biodegradation of TNT using whey as an electron donor: a case study. N. Biotechnol. 32, 701–709. https://doi.org/10.1016/j.nbt.2015.03.014

Khan, I.A., Spalding, R.F., 2004. Enhanced in situ denitrification for a municipal well. Water Res. 38, 3382–3388. https://doi.org/10.1016/j.watres.2004.04.052

Knowles, R., 1982. Denitrification. Microbiol. Rev. 46, 43–70.

Korom, S.F., 1992. Natural denitrification in the saturated zone: A review. Water Resour. Res. 28, 1657–1668. https://doi.org/10.1029/92WR00252

Laverman, A.M., Pallud, C., Abell, J., Cappellen, P. Van, 2012. Comparative survey of

potential nitrate and sulfate reduction rates in aquatic sediments. Geochim. Cosmochim. Acta 77, 474–488. https://doi.org/10.1016/j.gca.2011.10.033

Leverenz, H.L., Haunschild, K., Hopes, G., Tchobanoglous, G., Darby, J.L., 2010. Anoxic treatment wetlands for denitrification. Ecol. Eng. 36, 1544–1551. https://doi.org/10.1016/j.ecoleng.2010.03.014

Lin, Y.F., Jing, S.R., Wang, T.W., Lee, D.Y., 2002. Effects of macrophytes and external carbon sources on nitrate removal from groundwater in constructed wetlands. Environ. Pollut. 119, 413–420. https://doi.org/10.1016/S0269-7491(01)00299-8

Mariotti, A., 1991. Le carbone 13 en abondance naturelle, traceur de la dynamique de la matière organique des sols et de l'évolution des paléoenvironnements continentaux. Cah. Orstom, sér. Pédol. XXVI, 299–313.

Mariotti, A., Landreau, A., Simon, B., 1988. ^{15}N isotope biogeochemistry and natural denitrification process in groundwater: Application to the chalk aquifer of northern France. Geochim. Cosmochim. Acta 52, 1869–1878. https://doi.org/10.1016/0016-7037(88)90010-5

McIlvin, M.R., Altabet, M.A., 2005. Chemical conversion of nitrate and nitrite to nitrous oxide for nitrogen and oxygen isotopic analysis in freshwater and seawater. Anal Chem 77, 5589–5595. https://doi.org/10.1021/ac050528s

Mclean, J.E., Ervin, J., Zhou, J., Sorensen, D.L., Dupont, R.R., 2015. Biostimulation and Bioaugmentation to Enhance Reductive Dechlorination of TCE in a Long-Term Flow Through Column Study. Groundw. Monit. Remediat. 35, 76–88. https://doi.org/10.1111/gwmr.12113

Miettinen, H., Pumpanen, J., Heiskanen, J.J., 2015. Towards a more comprehensive understanding of lacustrine greenhouse gas dynamics — two-year measurements of concentrations and fluxes of CO_2, CH_4 and N_2O in a typical boreal lake

surrounded by managed forests. Boreal Environ. Res. 20, 75–89.

Nascimento, C., Krishnamurthy, R. V, 1997. Inorganic Carbon in Denitrifying Environments Investigation. Geophys. Res. Lett. 24, 1511–1514.

Němeček, J., Pokorný, P., Lacinová, L., Černík, M., Masopustová, Z., Lhotský, O., Filipová, A., Cajthaml, T., 2015. Combined abiotic and biotic in-situ reduction of hexavalent chromium in groundwater using nZVI and whey: A remedial pilot test. J. Hazard. Mater. 300, 670–679. https://doi.org/10.1016/j.jhazmat.2015.07.056

Oliveira, C.P., Gloria, M.B. a, Barbour, J.F., Scanlan, R. a, 1995. Nitrate, nitrite, and volatile nitrosamines in whey-containing food products. J. Agric. Food Chem. 43, 967–969. https://doi.org/10.1021/jf00052a023

Orozco, A.M.F., Contreras, E.M., Zaritzky, N.E., 2010. Cr(VI) reduction capacity of activated sludge as affected by nitrogen and carbon sources, microbial acclimation and cell multiplication. J. Hazard. Mater. 176, 657–665. https://doi.org/10.1016/j.jhazmat.2009.11.082

Otero, N., Torrentó, C., Soler, A., Menció, A., Mas-Pla, J., 2009. Monitoring groundwater nitrate attenuation in a regional system coupling hydrogeology with multi-isotopic methods: The case of Plana de Vic (Osona, Spain). Agric. Ecosyst. Environ. 133, 103–113. https://doi.org/10.1016/j.agee.2009.05.007

Peng, Y.Z., Ma, Y., Wang, S.Y., 2007. Denitrification potential enhancement by addition of external carbon sources in a pre-denitrification process. J. Environ. Sci. 19, 284–289. https://doi.org/10.1016/S1001-0742(07)60046-1

Rivett, M.O., Buss, S.R., Morgan, P., Smith, J.W.N., Bemment, C.D., 2008. Nitrate attenuation in groundwater: A review of biogeochemical controlling processes. Water Res. 42, 4215–4232. https://doi.org/10.1016/j.watres.2008.07.020

Robertson, W.D., Vogan, J.L., Lombardo, P.S., 2008. Nitrate Removal Rates in a 15

Year Old Permeable Reactive Barrier Treating Septic System Nitrate. Ground Water Monit. Remediat. 28, 65–72.

Rodríguez-Escales, P., Folch, A., Vidal-Gavilan, G., van Breukelen, B.M., 2016. Modeling biogeochemical processes and isotope fractionation of enhanced in situ biodenitrification in a fractured aquifer. Chem. Geol. 425, 52–64. https://doi.org/10.1016/j.chemgeo.2016.01.019

Ryabenko, E., Altabet, M. a., Wallace, D.W.R., 2009. Effect of chloride on the chemical conversion of nitrate to nitrous oxide for $\delta^{15}N$ analysis. Limnol. Oceanogr. Methods 7, 545–552. https://doi.org/10.4319/lom.2009.7.545

Safonov, A. V., Babich, T.L., Sokolova, D.S., Grouzdev, D.S., Tourova, T.P., Poltaraus, A.B., Zakharova, E. V., Merkel, A.Y., Novikov, A.P., Nazina, T.N., 2018. Microbial community and in situ bioremediation of groundwater by nitrate removal in the zone of a radioactive waste surface repository. Front. Microbiol. 9, 1–17. https://doi.org/10.3389/fmicb.2018.01985

Sage, M., Daufin, G., Gésan-Guiziou, G., 2006. Denitrification potential and rates of complex carbon source from dairy effluents in activated sludge system. Water Res. 40, 2747–2755. https://doi.org/10.1016/j.watres.2006.04.005

Salminen, J.M., Petäjäjärvi, S.J., Tuominen, S.M., Nystén, T.H., 2014. Ethanol-based in situ bioremediation of acidified, nitrate-contaminated groundwater. Water Res. 63, 306–315. https://doi.org/10.1016/j.watres.2014.06.013

Sebilo, M., Mayer, B., Nicolardot, B., Pinay, G., Mariotti, A., 2013. Long-term fate of nitrate fertilizer in agricultural soils. Proc. Natl. Acad. Sci. U. S. A. 110, 18185–9. https://doi.org/10.1073/pnas.1305372110

Smith, R.L., Miller, D.N., Brooks, M.H., Widdowson, M.A., Killingstad, M.W., 2001. In situ stimulation of groundwater denitrification with formate to remediate nitrate

contamination. Environ. Sci. Technol. 35, 196–203. https://doi.org/10.1021/es001360p

Spoelstra, J., Schiff, S.L., Semkin, R.G., Jeffries, D.S., Elgood, R.J., 2010. Nitrate attenuation in a small temperate wetland following forest harvest. For. Ecol. Manage. 259, 2333–2341. https://doi.org/10.1016/j.foreco.2010.03.006

Tang, J., Wang, X.C., Hu, Y., Pu, Y., Huang, J., Hao Ngo, H., Zeng, Y., Li, Y., 2018. Nitrogen removal enhancement using lactic acid fermentation products from food waste as external carbon sources: Performance and microbial communities. Bioresour. Technol. 256, 259–268. https://doi.org/10.1016/j.biortech.2018.02.033

Tartakovsky, B., Millette, D., Del Isle, S., Guiot, S.R., 2002. Ethanol-stimulated bioremediation of nitrate-contaminated ground water. Gr. Water Monit. Remediat. https://doi.org/10.1111/j.1745-6592.2002.tb00656.x

Teiter, S., Mander, Ü., 2005. Emission of N_2O, N_2, CH_4, and CO_2 from constructed wetlands for wastewater treatment and from riparian buffer zones. Ecol. Eng. 25, 528–541. https://doi.org/10.1016/j.ecoleng.2005.07.011

Trois, C., Pisano, G., Oxarango, L., 2010. Alternative solutions for the bio-denitrification of landfill leachates using pine bark and compost. J. Hazard. Mater. 178, 1100–1105. https://doi.org/10.1016/j.jhazmat.2010.01.054

Vidal-Gavilan, G., Carrey, R., Solanas, A., Soler, A., 2014. Feeding strategies for groundwater enhanced biodenitrification in an alluvial aquifer: Chemical, microbial and isotope assessment of a 1D flow-through experiment. Sci. Total Environ. 494–495, 241–251. https://doi.org/10.1016/j.scitotenv.2014.06.100

Vidal-Gavilan, G., Folch, A., Otero, N., Solanas, A.M., Soler, A., 2013. Isotope characterization of an in situ biodenitrification pilot-test in a fractured aquifer. Appl. Geochemistry 32, 153–163. https://doi.org/10.1016/j.apgeochem.2012.10.033

Vitousek, P.M., Aber, J.D., Howarth, R.W., Likens, G.E., Matson, P.A., Schindler, D.W., Schlesinger, W.H., Tilman, D.G., 1997. Human alteration of the global nitrogen cycle: Sources and consequences. Ecol. Appl. 7, 737–750. https://doi.org/10.1017/CBO9781107415324.004

Ward, M.H., deKok, T.M., Levallois, P., Brender, J., Gulis, G., Nolan, B.T., VanDerslice, J., 2005. Workgroup report: Drinking-water nitrate and health - Recent findings and research needs. Environ. Health Perspect. 113, 1607–1614. https://doi.org/10.1289/ehp.8043

Weymann, D., Geistlinger, H., Well, R., Von Der Heide, C., Flessa, H., 2010. Kinetics of N_2O production and reduction in a nitrate-contaminated aquifer inferred from laboratory incubation experiments. Biogeosciences 7, 1953–1972. https://doi.org/10.5194/bg-7-1953-2010

WHO, 2011. Guidelines for Drinking-water Quality 4th ed., WHO, Geneva, p. 340. World Heal. Organ. https://doi.org/10.1016/S1462-0758(00)00006-6

Wunderlich, A., Meckenstock, R., Einsiedl, F., 2012. Effect of different carbon substrates on nitrate stable isotope fractionation during microbial denitrification. Environ. Sci. Technol. 46, 4861–4868. https://doi.org/10.1021/es204075b

Wunderlich, A., Meckenstock, R.U., Einsiedl, F., 2013. A mixture of nitrite-oxidizing and denitrifying microorganisms affects the $\delta^{18}O$ of dissolved nitrate during anaerobic microbial denitrification depending on the $\delta^{18}O$ of ambient water. Geochim. Cosmochim. Acta 119, 31–45. https://doi.org/10.1016/j.gca.2013.05.028

Ye, F., Ye, Y., Li, Y., 2011. Effect of C/N ratio on extracellular polymeric substances (EPS) and physicochemical properties of activated sludge flocs. J. Hazard. Mater. 188, 37–43. https://doi.org/10.1016/j.jhazmat.2011.01.043

Table 1. Experimental stages during the flow-through experiment. Tested C/N ratios and injection periodicities (IP).

STAGE	DAYS	C/N	IP
0	previous	0.0	NONE
I	0 to 24	3.0	4 days
II	24 to 77	0.0	NONE
III	77 to 99	2.0	1 day
IV	99 to 114	1.25	1 day
V	114 to 144	1.5	1 day
VI	144 to 170	0.0	NONE

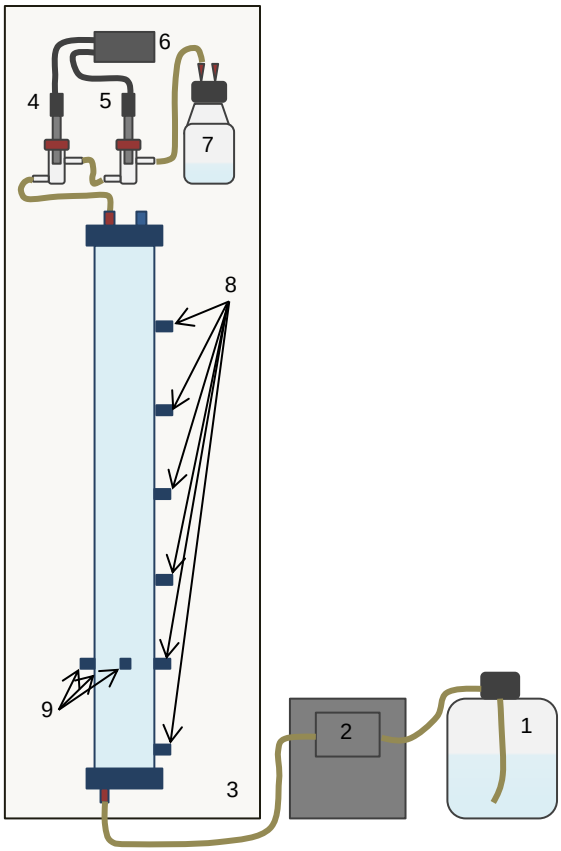

Figure 1. Scheme of the flow-through experimental design. Components: 1) inflow water, 2) peristaltic pump, 3) refrigerating chamber, 4) Eh probe, 5) pH probe, 6) multiparametric analyzer, 7) outflow water, 8) sampling points and 9) injection points.

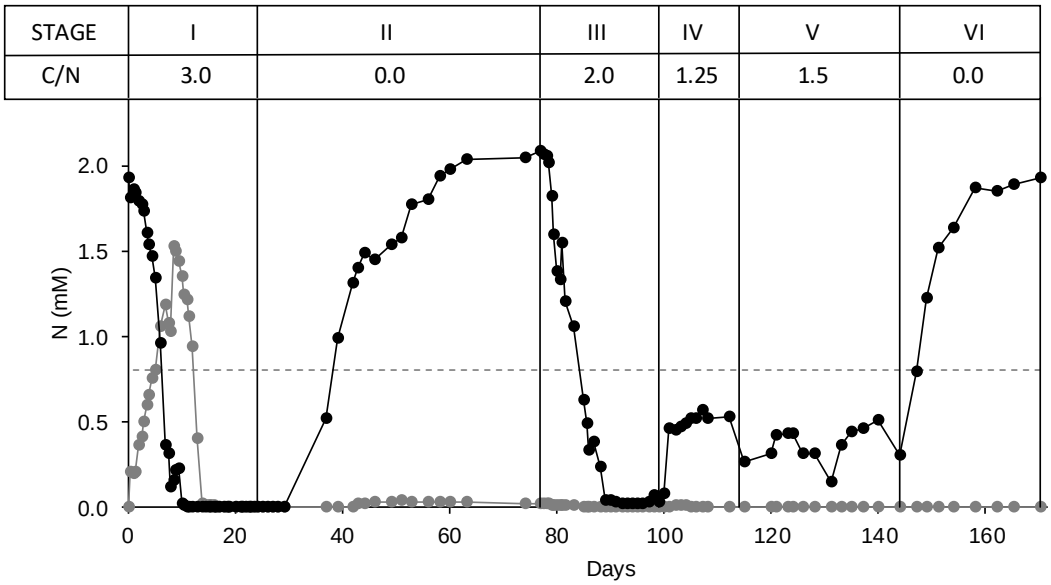

Figure 2. NO_3^- and NO_2^- evolution. NO_3^- (black dots) and NO_2^- (gray dots) concentration evolution throughout the biostimulation and recovery periods of the flow-through experiment (Stages I to VI). The black vertical lines depict the beginning and the end of each stage, while the gray dashed horizontal line depicts the NO_3^- threshold for water consumption.

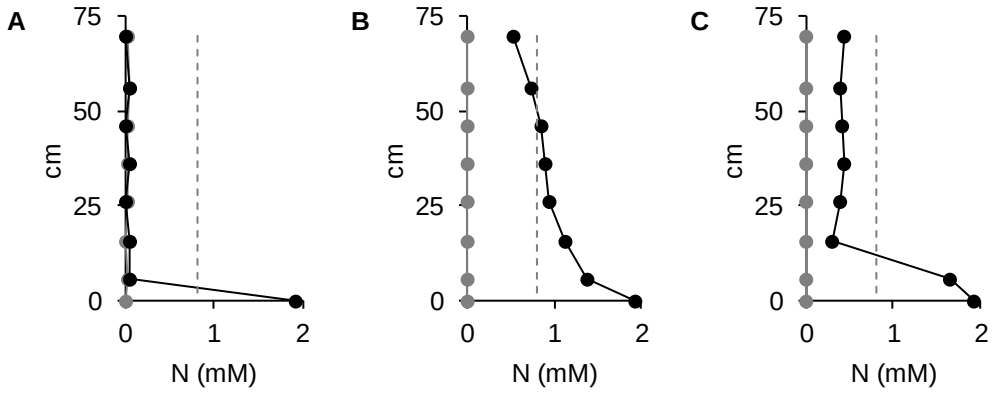

Figure 3. NO_3^- and NO_2^- vertical profile. NO_3^- (black dots) and NO_2^- (gray dots) concentration along the column. A) Stage I (C/N =3.0, day 16), B) Stage II (recovery, day 36) and C) Stage V (C/N = 1.5, day 136). The Y axis depicts the height of each sampling point with respect to the bottom of the column (**Figure 1**). The gray dashed line depicts the NO_3^- threshold for water consumption.

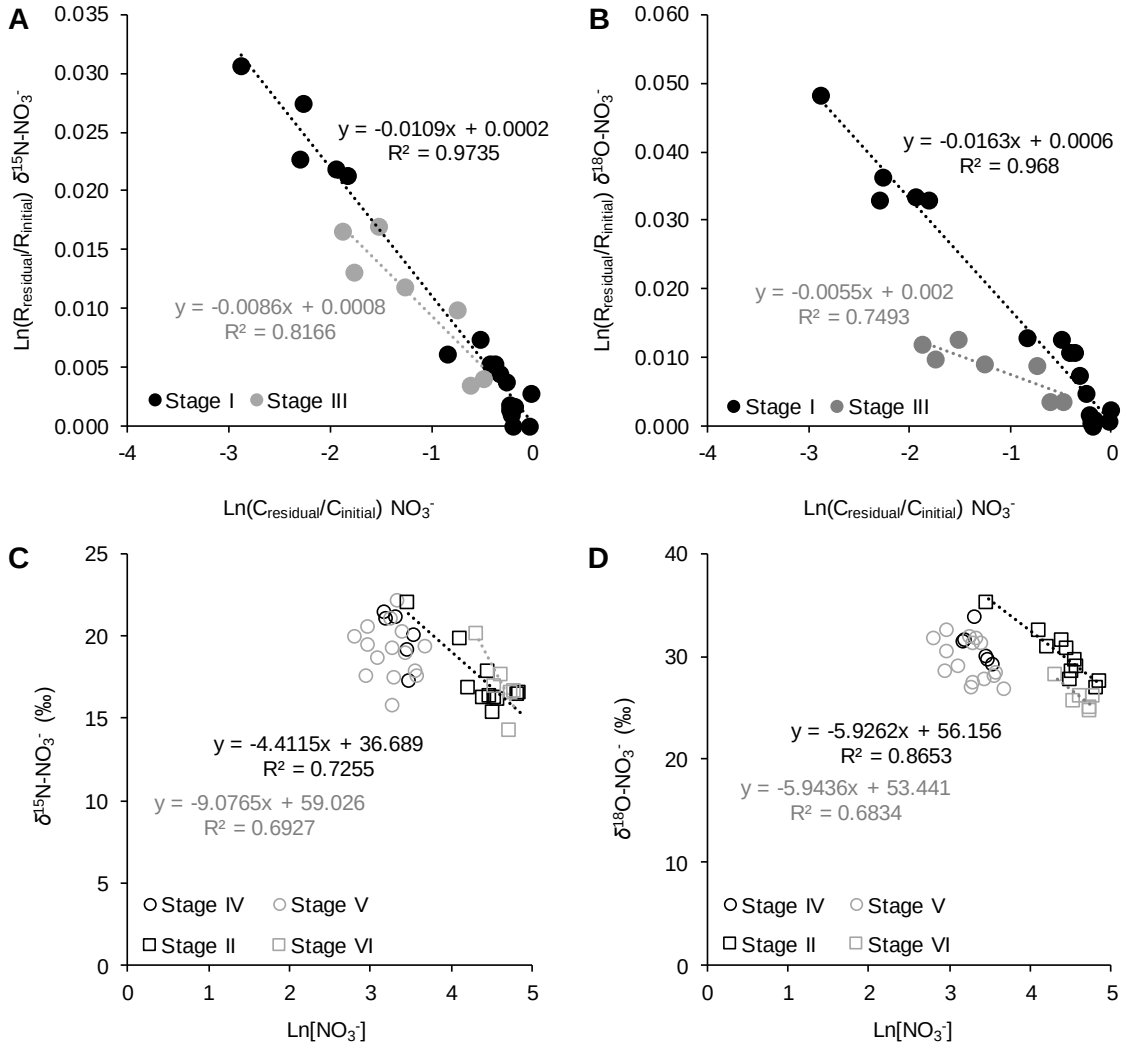

Figure 4. NO_3^- isotopic results. $\delta^{15}N\text{-}NO_3^-$ and $\delta^{18}O\text{-}NO_3^-$ composition versus concentration plots, including the regression line for complete denitrification stages (A and B) and partial denitrification and recovery stages (C and D). For plots A and B, the Rayleigh equation is used (**Equation 1**). No regression line is presented for the partial denitrification periods.

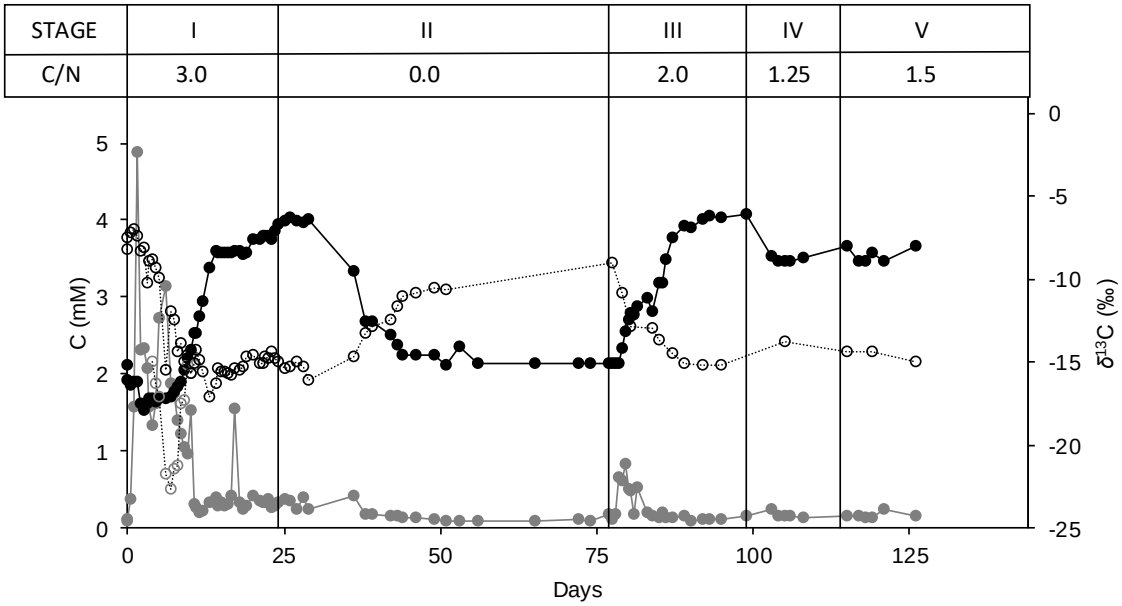

Figure 5. DIC and NPDOC concentration and isotopic composition evolution. Concentration (full circles) and $\delta^{13}C$ (empty circles) evolution of NPDOC (gray) and DIC (black) throughout the biostimulation and recovery periods of the flow-through experiment (Stages I to V). The black vertical lines depict the beginning and the end of each stage.

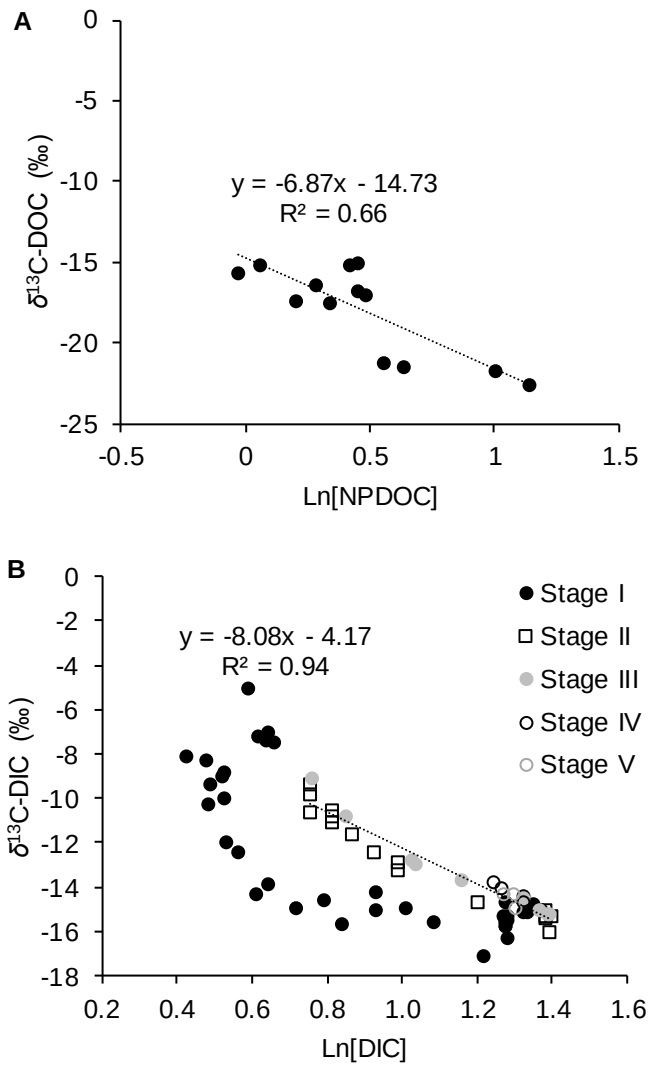

Figure 6. NPDOC and DIC isotopic composition versus concentration. A) For NPDOC, only results for Stage I were available. B) For DIC, samples from Stages I to V were analyzed.

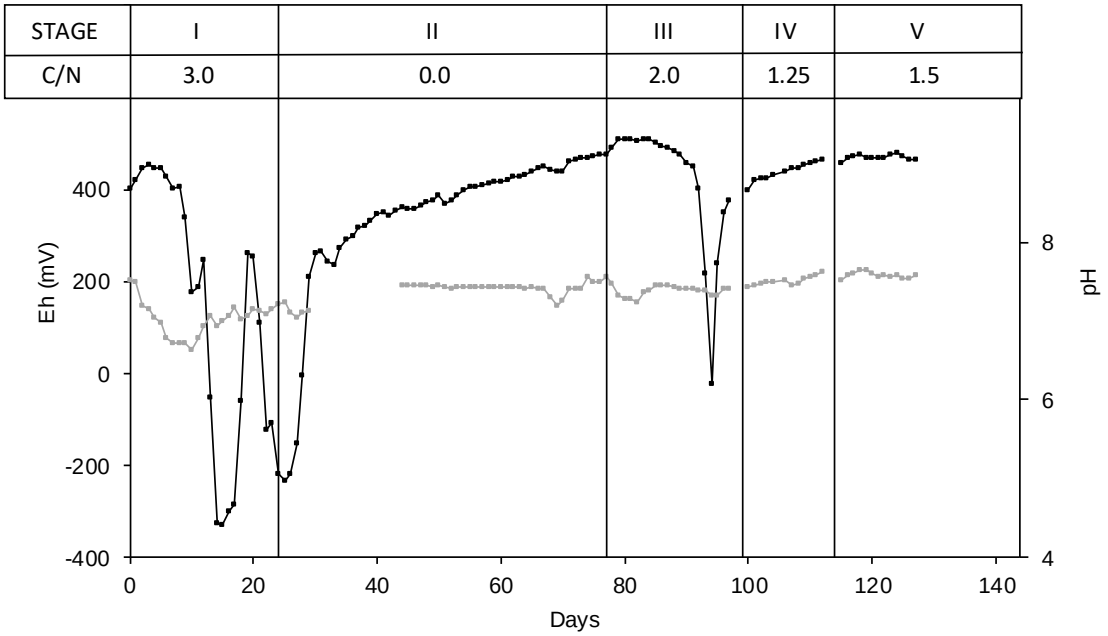

Figure S1. Eh and pH evolution. Eh (black dots) and pH (gray dots) values from the beginning of biostimulation at Stage I until the middle of Stage V. The black vertical lines depict the beginning and the end of each stage.

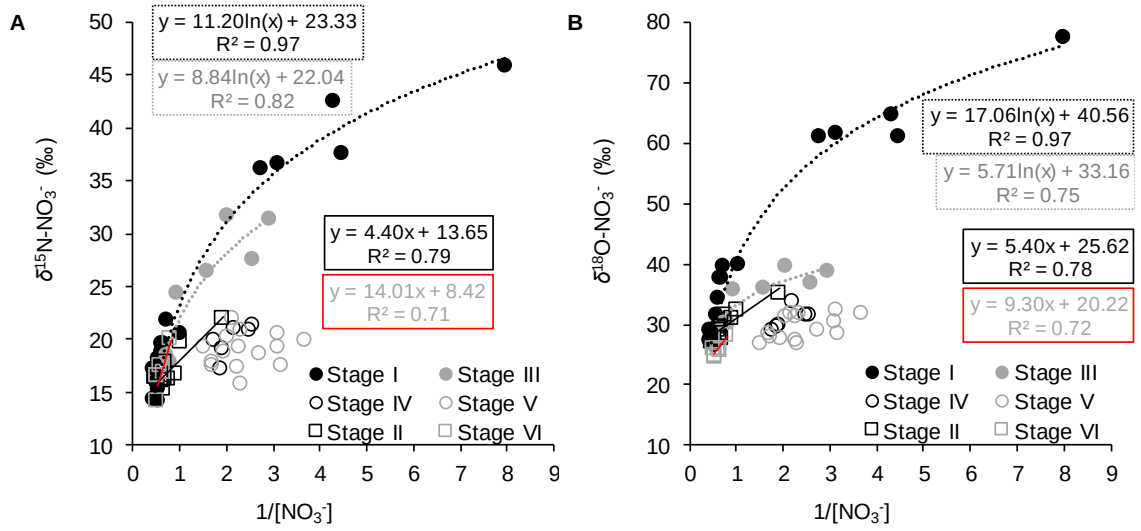

Figure S2. NO_3^- isotopic composition versus 1/[NO_3^-] plots. δ^{15}N-NO_3^- (A) and δ^{18}O-NO_3^- (B) for each stage against 1/[NO_3^-]. Stage I and III correspond to complete denitrification periods, Stage IV and V to partial denitrification periods and Stage II and VI to recovery periods. The correlation for the logarithmic trend obtained for Stage I and III is presented as dashed lines, while the linear trend for Stage II and VI is presented as continuous lines.

Table S1. Inflow water composition. Concentration of the reagents employed in the preparation of the synthetic water.

Chemical	mM
$CHNaO_3$	1.80
KH_2PO_4	0.03
$MgCl_2 \cdot 6H_2O$	1.25
KCl	1.45
$CaCl_2 \cdot 2H_2O$	0.85
Na_2SO_4	1.45
$NaNO_3$	1.90

Table S2. N and C compounds chemical and isotopic results. Measured concentration and isotopic composition of the N and C compounds from the samples collected throughout the flow-through experiment. “n.a.” refers to samples that were not analyzed.

		NO_3^- (mM)	NO_2^- (mM)	NH_4^+ (mM)	$\delta^{15}N\text{-}NO_3^-$ (‰)	SD ($\delta^{15}N\text{-}NO_3^-$)	$\delta^{18}O\text{-}NO_3^-$ (‰)	SD ($\delta^{18}O\text{-}NO_3^-$)	DIC (mM)	NPDOC (mM)	$\delta^{13}C$-DIC (‰)	$\delta^{13}C$-DOC (‰)
	DAY	SAMPLES COLLECTED AT THE OUTLET										
STAGE I	0.0	1.9	0.0	n.a.	14.4	0.1	27.2	1.5	1.9	0.1	-7.5	n.a.
	0.5	1.8	0.2	n.a.	15.3	0.1	27.2	0.2	1.8	0.1	-7.2	n.a.
	1.0	1.9	0.2	n.a.	16.0	0.1	27.5	0.0	1.9	0.4	-7.0	n.a.
	1.5	1.8	0.2	n.a.	14.3	0.1	26.5	0.1	1.9	1.6	-7.4	n.a.
	2.0	1.8	0.4	n.a.	15.7	0.0	27.7	0.0	1.6	4.9	-8.3	n.a.
	2.5	1.8	0.4	n.a.	16.1	0.0	28.4	0.5	1.5	2.3	-8.1	n.a.
	3.0	1.7	0.5	n.a.	18.2	0.4	31.4	0.7	1.6	2.3	-10.2	n.a.
	3.5	1.6	0.6	0.1	18.8	0.0	34.2	0.6	1.7	2.1	-8.9	n.a.
	4.0	1.5	0.7	n.a.	19.7	0.1	37.6	0.6	1.7	1.6	-8.8	-15.0
	4.5	1.5	0.8	n.a.	19.6	0.2	37.7	0.4	1.6	1.3	-9.3	-16.3
	5.0	1.3	0.8	n.a.	21.8	0.1	39.6	0.3	1.7	1.6	-9.9	-17.0
	6.0	1.0	1.1	0.0	20.5	0.2	40.0	0.2	1.7	2.7	-15.4	-21.7
	7.0	0.4	1.2	n.a.	36.1	0.1	60.9	0.9	1.7	3.1	-12.0	-22.6
	7.5	0.3	1.1	0.0	36.7	0.3	61.5	0.3	1.8	1.9	-12.4	-21.4
	8.0	0.1	1.0	n.a.	45.8	0.5	77.3	0.0	1.8	1.7	-14.3	-21.2
	8.5	0.2	1.5	n.a.	n.a.	n.a.	n.a.	n.a.	1.9	1.4	-13.9	-17.5
	9.0	0.2	1.5	n.a.	37.6	0.3	61.1	0.2	2.1	1.2	-14.9	-17.3
	9.5	0.2	1.4	n.a.	42.5	0.2	64.5	0.1	2.2	1.1	-14.6	-15.2
	10.0	0.0	1.4	n.a.	n.a.	n.a.	n.a.	n.a.	2.3	1.0	-15.7	-15.6
	10.5	0.0	1.2	n.a.	n.a.	n.a.	n.a.	n.a.	2.5	1.5	-15.0	-15.1

	11.0	0.0	1.2	n.a.	n.a.	n.a.	n.a.	n.a.	2.5	0.3	-14.2	n.a.
	11.5	0.0	1.1	0.0	n.a.	n.a.	n.a.	n.a.	2.7	0.3	-14.9	n.a.
	12.0	0.0	0.9	n.a.	n.a.	n.a.	n.a.	n.a.	3.0	0.2	-15.5	n.a.
	13.0	0.0	0.4	n.a.	n.a.	n.a.	n.a.	n.a.	3.4	0.2	-17.1	n.a.
	14.0	0.0	0.0	n.a.	n.a.	n.a.	n.a.	n.a.	3.6	0.3	-16.3	n.a.
	14.5	0.0	0.0	n.a.	n.a.	n.a.	n.a.	n.a.	3.6	0.4	-15.4	n.a.
	15.0	0.0	0.0	n.a.	n.a.	n.a.	n.a.	n.a.	3.6	0.3	-15.5	n.a.
	15.5	0.0	0.0	n.a.	n.a.	n.a.	n.a.	n.a.	3.6	0.3	-15.5	n.a.
	16.0	0.0	0.0	0.1	n.a.	n.a.	n.a.	n.a.	3.6	0.3	-15.7	n.a.
	16.5	0.0	0.0	n.a.	n.a.	n.a.	n.a.	n.a.	3.6	0.3	-15.8	n.a.
	17.0	0.0	0.0	n.a.	n.a.	n.a.	n.a.	n.a.	3.6	n.a.	-15.3	n.a.
	18.0	0.0	0.0	n.a.	n.a.	n.a.	n.a.	n.a.	3.6	0.4	-15.5	n.a.
	18.5	0.0	0.0	n.a.	n.a.	n.a.	n.a.	n.a.	3.6	1.6	-15.3	-16.7
	19.0	0.0	0.0	n.a.	n.a.	n.a.	n.a.	n.a.	3.6	0.3	-14.7	n.a.
	20.0	0.0	0.0	0.0	n.a.	n.a.	n.a.	n.a.	3.8	0.3	-14.6	n.a.
	21.0	0.0	0.0	n.a.	n.a.	n.a.	n.a.	n.a.	3.8	0.3	-15.1	n.a.
	21.5	0.0	0.0	n.a.	n.a.	n.a.	n.a.	n.a.	3.8	0.4	-15.1	n.a.
	22.0	0.0	0.0	n.a.	n.a.	n.a.	n.a.	n.a.	3.8	0.3	-14.7	n.a.
	22.5	0.0	0.0	n.a.	n.a.	n.a.	n.a.	n.a.	3.8	0.3	-14.7	n.a.
	23.0	0.0	0.0	n.a.	n.a.	n.a.	n.a.	n.a.	3.8	0.3	-14.4	n.a.
	23.5	0.0	0.0	n.a.	n.a.	n.a.	n.a.	n.a.	3.8	0.4	-14.8	n.a.
	24.0	0.0	0.0	n.a.	n.a.	n.a.	n.a.	n.a.	3.9	0.3	-15.0	n.a.
	25.0	0.0	0.0	n.a.	n.a.	n.a.	n.a.	n.a.	4.0	0.3	-15.4	n.a.
	26.0	0.0	0.0	n.a.	n.a.	n.a.	n.a.	n.a.	4.0	0.3	-15.3	n.a.
STAGE II	27.0	0.0	0.0	n.a.	n.a.	n.a.	n.a.	n.a.	4.0	0.4	-15.0	n.a.
	28.0	0.0	0.0	n.a.	n.a.	n.a.	n.a.	n.a.	4.0	0.4	-15.2	n.a.
	29.0	0.0	0.0	0.0	n.a.	n.a.	n.a.	n.a.	4.0	0.2	-16.0	n.a.

	36.0	0.5	0.0	0.2	22.0	0.2	35.1	0.1	3.3	0.4	-14.7	n.a.
	38.0	1.1	0.0	n.a.	16.8	0.0	30.9	0.1	2.7	0.3	-13.2	n.a.
	39.0	1.0	0.0	n.a.	19.8	0.1	32.4	1.0	2.7	0.4	-12.9	n.a.
	42.0	1.3	0.0	n.a.	16.3	0.7	31.5	0.3	2.5	0.2	-12.4	n.a.
	43.0	1.4	0.0	n.a.	17.8	0.5	30.7	0.5	2.4	0.2	-11.6	n.a.
	44.0	1.5	0.0	0.1	15.3	0.2	28.5	0.3	2.3	0.2	-11.0	n.a.
	46.0	1.4	0.0	n.a.	16.3	0.1	27.7	0.2	2.3	0.2	-10.8	n.a.
	49.0	1.5	0.0	n.a.	16.3	0.6	29.6	1.0	2.3	0.1	-10.5	n.a.
	51.0	1.6	0.0	n.a.	16.1	0.2	29.0	0.8	2.1	0.1	-10.6	n.a.
	53.0	1.8	0.0	n.a.	n.a.	n.a.	n.a.	n.a.	2.3	0.1	n.a.	n.a.
	56.0	1.8	0.0	n.a.	n.a.	n.a.	n.a.	n.a.	2.1	0.1	n.a.	n.a.
	58.0	1.9	0.0	n.a.	n.a.	n.a.	n.a.	n.a.	2.1	0.1	-9.8	n.a.
	60.0	2.0	0.0	n.a.	n.a.	n.a.	n.a.	n.a.	n.a.	0.1	n.a.	n.a.
	63.0	2.0	0.0	0.0	16.4	0.2	27.0	1.0	2.1	0.1	-9.3	n.a.
	65.0	1.7	0.0	n.a.	n.a.	n.a.	n.a.	n.a.	2.1	0.1	n.a.	n.a.
	72.0	1.4	0.0	n.a.	n.a.	n.a.	n.a.	n.a.	2.1	0.1	n.a.	n.a.
	74.0	2.1	0.0	n.a.	n.a.	n.a.	n.a.	n.a.	2.1	0.2	n.a.	n.a.
	77.0	2.1	0.0	n.a.	16.5	1.0	27.5	0.2	2.1	n.a.	n.a.	n.a.
STAGE III	77.5	2.1	0.0	n.a.	n.a.	n.a.	n.a.	n.a.	2.1	0.1	-9.0	n.a.
	78.0	2.1	0.0	0.0	n.a.	n.a.	n.a.	n.a.	2.1	0.2	n.a.	n.a.
	78.5	2.0	0.0	0.0	n.a.	n.a.	n.a.	n.a.	2.1	0.7	n.a.	n.a.
	79.0	1.8	0.0	n.a.	n.a.	n.a.	n.a.	n.a.	2.3	0.6	-10.8	n.a.
	79.5	1.6	0.0	n.a.	n.a.	n.a.	n.a.	n.a.	2.5	0.8	n.a.	n.a.
	80.0	1.4	0.0	0.0	18.4	0.6	30.3	0.2	2.7	0.5	n.a.	n.a.
	80.5	1.3	0.0	n.a.	n.a.	n.a.	n.a.	n.a.	2.8	0.5	-12.8	n.a.
	81.0	1.5	0.0	n.a.	n.a.	n.a.	n.a.	n.a.	2.8	0.2	n.a.	n.a.
	81.5	1.2	0.0	n.a.	17.9	0.3	30.2	0.2	2.9	0.5	n.a.	n.a.

	83.0	1.1	0.0	n.a.	24.4	0.1	35.6	0.8	3.0	0.2	n.a.	n.a.
	84.0	1.2	0.0	n.a.	n.a.	n.a.	n.a.	n.a.	2.8	0.2	-12.9	n.a.
	85.0	0.6	0.0	n.a.	26.4	0.9	35.9	0.8	3.2	0.1	-13.6	n.a.
	85.5	0.5	0.0	n.a.	31.7	0.3	39.6	0.4	3.2	0.2	n.a.	n.a.
	86.0	0.3	0.0	n.a.	31.3	0.9	38.9	1.1	3.5	0.1	n.a.	n.a.
	87.0	0.4	0.0	0.0	27.6	0.1	36.8	0.5	3.8	0.1	-14.5	n.a.
	88.0	0.2	0.0	n.a.	n.a.	n.a.	n.a.	n.a.	n.a.	0.2	n.a.	n.a.
	89.0	0.0	0.0	n.a.	n.a.	n.a.	n.a.	n.a.	3.9	0.1	-15.1	n.a.
	90.0	0.0	0.0	0.0	n.a.	n.a.	n.a.	n.a.	3.9	0.1	n.a.	n.a.
	91.0	0.0	0.0	n.a.	n.a.	n.a.	n.a.	n.a.	n.a.	0.1	n.a.	n.a.
	92.0	0.0	0.0	n.a.	n.a.	n.a.	n.a.	n.a.	4.0	0.1	-15.2	n.a.
	93.0	0.0	0.0	n.a.	n.a.	n.a.	n.a.	n.a.	4.1	0.2	n.a.	n.a.
	94.0	0.0	0.0	n.a.	n.a.	n.a.	n.a.	n.a.	n.a.	n.a.	n.a.	n.a.
	95.0	0.0	0.0	n.a.	n.a.	n.a.	n.a.	n.a.	4.0	0.2	-15.2	n.a.
	96.0	0.0	0.0	n.a.	n.a.	n.a.	n.a.	n.a.	n.a.	n.a.	n.a.	n.a.
	97.0	0.0	0.0	n.a.	n.a.	n.a.	n.a.	n.a.	n.a.	n.a.	n.a.	n.a.
	98.0	0.1	0.0	n.a.	n.a.	n.a.	n.a.	n.a.	n.a.	0.2	n.a.	n.a.
	99.0	0.0	0.0	n.a.	n.a.	n.a.	n.a.	n.a.	4.1	n.a.	n.a.	n.a.
STAGE IV	100.0	0.1	0.0	n.a.	n.a.	n.a.	n.a.	n.a.	3.8	n.a.	-14.6	n.a.
	101.0	0.5	0.0	n.a.	n.a.	n.a.	n.a.	n.a.	3.5	0.2	-14.0	n.a.
	102.0	0.4	0.0	0.0	n.a.	n.a.	n.a.	n.a.	n.a.	n.a.	n.a.	n.a.
	103.0	0.5	0.0	n.a.	n.a.	n.a.	n.a.	n.a.	3.5	0.2	n.a.	n.a.
	104.0	0.5	0.0	n.a.	n.a.	n.a.	n.a.	n.a.	3.5	0.1	n.a.	n.a.
	105.0	0.5	0.0	n.a.	n.a.	n.a.	n.a.	n.a.	3.5	0.2	-13.8	n.a.
	106.0	0.5	0.0	n.a.	n.a.	n.a.	n.a.	n.a.	3.5	0.2	n.a.	n.a.
	107.0	0.6	0.0	n.a.	20.0	0.2	29.1	0.6	n.a.	n.a.	n.a.	n.a.
	108.0	0.5	0.0	n.a.	19.1	0.2	29.9	0.4	3.5	n.a.	n.a.	n.a.

	109.0	0.4	0.0	n.a.	21.3	0.0	31.4	0.2	n.a.	0.1	n.a.	n.a.
	110.0	0.4	0.0	n.a.	21.0	0.2	31.5	0.5	n.a.	n.a.	n.a.	n.a.
	111.0	0.5	0.0	n.a.	21.1	0.5	33.7	0.4	n.a.	n.a.	n.a.	n.a.
	112.0	0.5	0.0	n.a.	17.2	n.a.	29.6	n.a.	n.a.	0.1	n.a.	n.a.
STAGE V	115.0	0.3	0.0	n.a.	19.9	0.3	31.7	0.2	3.7	n.a.	-14.3	n.a.
	116.0	0.6	0.0	n.a.	17.8	0.1	28.0	0.3	n.a.	n.a.	n.a.	n.a.
	117.0	0.6	0.0	n.a.	17.5	0.1	28.4	0.4	3.5	0.3	n.a.	n.a.
	118.0	0.7	0.0	n.a.	n.a.	n.a.	n.a.	n.a.	3.5	0.2	n.a.	n.a.
	119.0	0.5	0.0	n.a.	20.2	0.0	31.2	0.0	3.6	0.2	-14.3	n.a.
	120.0	0.3	0.0	n.a.	20.5	0.2	32.4	0.4	n.a.	n.a.	n.a.	n.a.
	121.0	0.4	0.0	n.a.	20.9	0.4	31.9	0.2	3.5	n.a.	n.a.	n.a.
	123.0	0.4	0.0	n.a.	15.7	0.8	26.9	0.0	n.a.	n.a.	n.a.	n.a.
	124.0	0.4	0.0	n.a.	19.2	0.4	31.2	0.0	n.a.	n.a.	n.a.	n.a.
	126.0	0.3	0.0	n.a.	19.4	0.9	30.4	0.6	3.7	n.a.	-14.9	n.a.
	128.0	0.3	0.0	n.a.	17.5	0.1	28.4	0.4	n.a.	n.a.	n.a.	n.a.
	131.0	0.2	0.0	n.a.	n.a.	n.a.	n.a.	n.a.	n.a.	n.a.	n.a.	n.a.
	133.0	0.4	0.0	n.a.	18.6	0.4	29.0	0.5	n.a.	n.a.	n.a.	n.a.
	135.0	0.4	0.0	n.a.	17.4	0.1	27.3	0.3	n.a.	n.a.	n.a.	n.a.
	137.0	0.5	0.0	n.a.	22.1	0.0	31.7	0.2	n.a.	n.a.	n.a.	n.a.
	140.0	0.5	0.0	n.a.	18.9	0.9	27.7	0.5	n.a.	n.a.	n.a.	n.a.
	141.0	0.7	0.0	n.a.	19.3	0.2	26.8	0.4	n.a.	n.a.	n.a.	n.a.
	144.0	0.3	0.0	n.a.	n.a.	n.a.	n.a.	n.a.	n.a.	n.a.	n.a.	n.a.
STAGE VI	147.0	0.8	0.0	n.a.	n.a.	n.a.	n.a.	n.a.	n.a.	n.a.	n.a.	n.a.
	149.0	1.2	0.0	n.a.	20.1	0.3	28.2	0.5	n.a.	n.a.	n.a.	n.a.
	151.0	1.5	0.0	n.a.	16.9	0.3	25.6	0.0	n.a.	n.a.	n.a.	n.a.
	154.0	1.6	0.0	n.a.	17.6	0.6	26.1	0.1	n.a.	n.a.	n.a.	n.a.
	158.0	1.9	0.0	n.a.	16.5	0.2	24.9	0.5	n.a.	n.a.	n.a.	n.a.

	162.0	1.8	0.0	n.a.	14.3	0.3	24.7	0.0	n.a.	n.a.	n.a.	n.a.
	165.0	1.9	0.0	n.a.	n.a.	n.a.	n.a.	n.a.	n.a.	n.a.	n.a.	n.a.
	170.0	1.9	0.0	n.a.	16.6	0.3	26.1	0.1	n.a.	n.a.	n.a.	n.a.
	cm	SAMPLES FROM THE VERTICAL PROFILES										
STAGE I (day 16)	06.0	0.0	0.0	n.a.	n.a.	n.a.	n.a.	n.a.	n.a.	n.a.	n.a.	n.a.
	16.0	0.1	0.0	n.a.	n.a.	n.a.	n.a.	n.a.	n.a.	n.a.	n.a.	n.a.
	26.0	0.0	0.0	n.a.	n.a.	n.a.	n.a.	n.a.	n.a.	n.a.	n.a.	n.a.
	36.0	0.0	0.0	n.a.	n.a.	n.a.	n.a.	n.a.	n.a.	n.a.	n.a.	n.a.
	46.0	0.0	0.0	n.a.	n.a.	n.a.	n.a.	n.a.	n.a.	n.a.	n.a.	n.a.
	56.0	0.0	0.0	n.a.	n.a.	n.a.	n.a.	n.a.	n.a.	n.a.	n.a.	n.a.
STAGE II (day 36)	06.0	1.4	0.0	n.a.	n.a.	n.a.	n.a.	n.a.	n.a.	n.a.	n.a.	n.a.
	16.0	1.1	0.0	n.a.	n.a.	n.a.	n.a.	n.a.	n.a.	n.a.	n.a.	n.a.
	26.0	0.9	0.0	n.a.	n.a.	n.a.	n.a.	n.a.	n.a.	n.a.	n.a.	n.a.
	36.0	0.9	0.0	n.a.	n.a.	n.a.	n.a.	n.a.	n.a.	n.a.	n.a.	n.a.
	46.0	0.8	0.0	n.a.	n.a.	n.a.	n.a.	n.a.	n.a.	n.a.	n.a.	n.a.
	56.0	0.7	0.0	n.a.	n.a.	n.a.	n.a.	n.a.	n.a.	n.a.	n.a.	n.a.
STAGE V (day 136)	06.0	1.7	0.0	n.a.	n.a.	n.a.	n.a.	n.a.	n.a.	n.a.	n.a.	n.a.
	16.0	0.3	0.0	n.a.	n.a.	n.a.	n.a.	n.a.	n.a.	n.a.	n.a.	n.a.
	26.0	0.4	0.0	n.a.	n.a.	n.a.	n.a.	n.a.	n.a.	n.a.	n.a.	n.a.
	36.0	0.4	0.0	n.a.	n.a.	n.a.	n.a.	n.a.	n.a.	n.a.	n.a.	n.a.
	46.0	0.4	0.0	n.a.	n.a.	n.a.	n.a.	n.a.	n.a.	n.a.	n.a.	n.a.
	56.0	0.4	0.0	n.a.	n.a.	n.a.	n.a.	n.a.	n.a.	n.a.	n.a.	n.a.

Table S3. ICP results. Concentration of the major cations and trace elements measured by ICP-OES (ppm) and ICP-MS (ppb), respectively.

		STAGE I										STAGE II		
	DAY	0.0	2.0	4.0	7.0	8.0	9.5	12.0	16.0	21.0	24.0	36.0	49.0	63.0
ICP-OES (ppm)	K	176.4	100.1	96.9	83.7	92.2	85.7	80.6	76.9	73.5	72.8	66.8	71.1	66.5
	Ca	40.0	39.1	39.0	39.1	42.6	42.5	39.8	38.5	38.8	37.1	37.4	36.0	37.1
	Mg	33.8	33.5	33.4	32.8	35.8	35.3	34.0	32.4	33.2	31.9	32.5	31.9	33.2
	S	58.1	56.6	55.7	57.0	59.9	58.9	57.2	56.8	51.1	48.0	47.2	46.3	46.9
	P	0.4	1.1	0.5	0.7	0.7	0.5	0.4	0.5	0.7	0.7	0.8	0.7	1.2
	Si	4.4	3.2	3.8	3.6	4.1	4.9	3.8	3.3	2.7	2.3	2.2	1.5	1.2
	B	0.2	0.1	0.1	0.1	0.1	0.1	0.1	0.1	0.1	0.0	0.0	0.0	0.0
	Zn	0.5	1.8	1.9	2.4	2.2	2.8	1.7	0.7	0.3	0.1	0.4	0.1	0.1
	Na	178.4	173.2	171.7	174.2	183.3	176.3	176.5	175.2	177.2	176.6	263.1	179.9	175.3
	Sr	0.1	0.0	0.0	0.0	0.0	0.0	0.0	0.0	0.0	0.0	0.0	0.0	0.0
ICP-MS (ppb)	Mn	7.3	14.0	12.7	32.5	33.9	55.1	42.6	21.4	22.6	2.1	3.2	3.0	0.7
	Fe	122.4	124.5	112.7	142.1	116.5	116.5	137.4	163.9	155.4	133.3	119.2	119.9	133.9
	Al	3.8	3.0	1.1	1.6	1.9	1.6	2.6	2.0	2.1	3.0	3.0	2.3	8.1
	Cu	4.1	5.2	3.9	7.3	6.3	7.1	14.9	10.7	3.1	4.1	20.7	2.5	2.0
	Tl	0.1	0.1	0.0	0.0	0.0	0.0	0.0	0.0	0.0	0.0	0.0	0.0	0.0
	Co	0.6	0.8	0.8	1.1	1.0	1.6	1.2	0.7	0.5	0.2	0.2	0.1	0.1
	Pb	0.4	0.1	0.4	0.1	0.1	0.1	0.7	0.2	0.2	0.1	0.7	0.1	0.1
	Sr	57.2	41.3	47.3	45.6	45.2	49.4	43.0	40.3	30.9	29.4	25.0	24.2	24.1
	Li	0.4	0.4	0.3	0.3	0.3	0.3	0.4	0.3	0.2	0.2	0.1	0.2	0.2
	Be	0.0	0.0	0.0	0.0	0.0	0.0	0.0	0.0	0.0	0.0	0.0	0.0	0.0
	Sc	1.4	1.0	1.2	1.2	1.1	1.3	1.2	1.1	0.7	0.7	0.6	0.4	0.3
	Ti	2.9	4.6	2.9	3.7	2.8	2.6	2.6	3.2	2.6	3.0	3.4	3.4	4.5

	V	1.0	1.1	1.2	1.4	1.5	1.5	1.5	1.5	1.5	1.5	1.4	1.3	1.4
	Cr	1.9	2.5	2.2	1.7	1.4	1.2	1.2	0.8	0.9	0.7	0.7	0.8	0.6
	Ni	3.7	4.4	4.3	4.7	5.3	6.6	5.5	4.8	2.2	1.2	4.6	1.4	1.0
	Ga	0.0	0.0	0.0	0.0	0.0	0.0	0.0	0.0	0.0	0.0	0.0	0.0	0.0
	Ge	0.0	0.0	0.0	0.0	0.0	0.0	0.0	0.0	0.0	0.0	0.0	0.0	0.0
	As	0.5	0.5	0.6	0.6	0.6	2.4	0.6	0.5	0.4	0.6	0.4	0.5	0.3
	Se	9.3	3.3	2.9	2.9	3.3	2.1	3.1	0.0	1.0	3.1	8.7	1.5	0.5
	Rb	5.0	5.9	4.6	6.4	5.3	5.5	6.0	6.6	5.5	5.9	4.1	2.4	2.0
	Y	0.0	0.0	0.0	0.1	0.1	0.1	0.1	0.0	0.0	0.0	0.0	0.0	0.0
	Zr	0.9	1.7	0.7	0.6	0.6	0.7	0.8	1.1	0.8	0.9	0.8	0.3	0.2
	Nb	0.0	0.0	0.0	0.0	0.0	0.0	0.0	0.0	0.0	0.0	0.0	0.0	0.0
	Mo	0.3	0.2	0.2	0.2	0.1	0.1	0.1	0.1	0.1	0.0	0.2	0.2	0.1
	Ru	0.0	0.0	0.0	0.0	0.0	0.0	0.0	0.0	0.0	0.0	0.0	0.0	0.0
	Rh	0.0	0.0	0.0	0.0	0.0	0.0	0.0	0.0	0.0	0.0	0.0	0.0	0.0
	Pd	0.1	0.0	0.0	0.0	0.0	0.0	0.0	0.0	0.0	0.0	0.0	0.0	0.0
	Ag	0.2	0.1	0.1	0.1	0.1	0.1	0.1	0.1	0.1	0.1	0.3	0.1	0.0
	Cd	0.9	1.1	1.0	1.4	1.5	1.2	0.6	0.2	0.1	0.1	0.1	0.1	0.0
	In	0.0	0.0	0.0	0.0	0.0	0.0	0.0	0.0	0.0	0.0	0.0	0.0	0.0
	Sn	0.5	0.1	0.0	0.0	0.0	0.1	0.1	0.1	0.0	0.1	0.5	0.0	0.0
	Sb	31.1	22.6	29.6	32.3	36.7	48.1	36.5	26.6	6.5	3.9	5.2	11.4	11.2
	Te	0.0	0.0	0.0	0.0	0.0	0.0	0.0	0.0	0.0	0.0	0.0	0.0	0.0
	Cs	0.1	0.0	0.0	0.0	0.0	0.0	0.0	0.0	0.0	0.0	0.0	0.0	0.0
	Ba	39.6	18.9	36.6	38.4	33.7	45.8	31.8	22.3	18.3	25.2	299.4	10.3	5.8
	La	0.0	0.0	0.0	0.0	0.0	0.0	0.0	0.0	0.0	0.0	0.0	0.0	0.0
	Ce	0.0	0.0	0.0	0.0	0.0	0.0	0.0	0.0	0.0	0.0	0.0	0.0	0.0
	Pr	0.0	0.0	0.0	0.0	0.0	0.0	0.0	0.0	0.0	0.0	0.0	0.0	0.0
	Nd	0.0	0.0	0.0	0.0	0.0	0.0	0.0	0.0	0.0	0.0	0.0	0.0	0.0

	Sm	0.0	0.0	0.0	0.0	0.0	0.0	0.0	0.0	0.0	0.0	0.0	0.0	0.0
	Eu	0.0	0.0	0.0	0.0	0.0	0.0	0.0	0.0	0.0	0.0	0.0	0.0	0.0
	Gd	0.0	0.0	0.0	0.0	0.0	0.0	0.0	0.0	0.0	0.0	0.0	0.0	0.0
	Tb	0.0	0.0	0.0	0.0	0.0	0.0	0.0	0.0	0.0	0.0	0.0	0.0	0.0
	Dy	0.0	0.0	0.0	0.0	0.0	0.0	0.0	0.0	0.0	0.0	0.0	0.0	0.0
	Ho	0.0	0.0	0.0	0.0	0.0	0.0	0.0	0.0	0.0	0.0	0.0	0.0	0.0
	Er	0.0	0.0	0.0	0.0	0.0	0.0	0.0	0.0	0.0	0.0	0.0	0.0	0.0
	Tm	0.0	0.0	0.0	0.0	0.0	0.0	0.0	0.0	0.0	0.0	0.0	0.0	0.0
	Yb	0.0	0.0	0.0	0.0	0.0	0.0	0.0	0.0	0.0	0.0	0.0	0.0	0.0
	Lu	0.0	0.0	0.0	0.0	0.0	0.0	0.0	0.0	0.0	0.0	0.0	0.0	0.0
	Hf	0.0	0.0	0.0	0.0	0.0	0.0	0.0	0.0	0.0	0.0	0.0	0.0	0.0
	Ta	0.0	0.0	0.0	0.0	0.0	0.0	0.0	0.0	0.0	0.0	0.0	0.0	0.0
	W	0.0	0.0	0.0	0.0	0.0	0.0	0.0	0.0	0.0	0.0	0.0	0.0	0.0
	Re	0.0	0.0	0.0	0.0	0.0	0.0	0.0	0.0	0.0	0.0	0.0	0.0	0.0
	Os	0.0	0.0	0.0	0.0	0.0	0.0	0.0	0.0	0.0	0.0	0.0	0.0	0.0
	Ir	0.0	0.0	0.0	0.0	0.0	0.0	0.0	0.0	0.0	0.0	0.0	0.0	0.0
	Pt	0.0	0.0	0.0	0.0	0.0	0.0	0.0	0.0	0.0	0.0	0.0	0.0	0.0
	Au	0.1	0.0	0.1	0.0	0.1	0.0	0.1	0.0	0.0	0.0	0.1	0.0	0.0
	Hg	0.3	0.2	0.2	0.1	0.1	0.2	0.1	0.0	0.0	0.0	0.2	0.0	0.0
	Bi	0.3	0.1	0.1	0.0	0.0	0.0	0.0	0.0	0.0	0.0	0.1	0.1	0.0
	Th	0.6	0.2	0.2	0.1	0.1	0.1	0.1	0.0	0.0	0.0	0.0	0.0	0.0
	U	0.1	0.1	0.1	0.1	0.0	0.0	0.1	0.1	0.1	0.1	0.1	0.0	0.0